

**İSTANBUL TECHNICAL UNIVERSITY ★ GRADUATE SCHOOL OF
SCIENCE ENGINEERING AND TECHNOLOGY**

EUTECTIC FREEZE CRYSTALLIZATION OF BORON COMPOUNDS

M.Sc. THESIS

Bolormaa BAYARKHUU

Department of Chemical Engineering

Chemical Engineering Programme

JUNE 2016

**İSTANBUL TECHNICAL UNIVERSITY ★ GRADUATE SCHOOL OF
SCIENCE ENGINEERING AND TECHNOLOGY**

EUTECTIC FREEZE CRYSTALLIZATION OF BORON COMPOUNDS

M.Sc. THESIS

**Bolormaa BAYARKHUU
(506121031)**

Department of Chemical Engineering

Chemical Engineering Programme

Thesis Advisor: Doç. Dr. F. Elif Genceli GÜNER

JUNE 2016

İSTANBUL TEKNİK ÜNİVERSİTESİ ★ FEN BİLİMLERİ ENSTİTÜSÜ

BOR BİRLEŞİKLERİN ÖTEKTİK DONDURMA KRİSTALİZASYONU

YÜKSEK LİSANS TEZİ

**Bolormaa BAYARKHUU
(506121031)**

Kimya Mühendisliği Anabilim Dalı

Kimya Mühendisliği Programı

Tez Danışmanı: Doç. Dr. F. Elif Genceli GÜNER

HAZİRAN 2016

Bolormaa BAYARKHUU, a **M.Sc.** student of ITU **Institute of Science and Technology** student ID **506121031**, successfully defended the **thesis** entitled **“EUTECTIC FREEZE CRYSTALLIZATION OF BORON COMPOUNDS”**, which she prepared after fulfilling the requirements specified in the associated legislations, before the jury whose signatures are below.

Thesis Advisor: **Doç. Dr. F. Elif Genceli GÜNER**

Istanbul Technical University

Jury Members: **Prof. Dr. Hale Gürbüz**

Istanbul Technical University

Doç. Dr. Didem Saloğlu Dertli

Yalova University

Date of Submission: 02 May 2016

Date of Defense: 28 June 2016

To my dear family,

FOREWORD

First, I particularly thank to honourable my thesis advisor Doç. Dr. F.Elif Genceli GÜNER for her guidance and giving chance to me perform my master thesis and also thank to Prof. Dr. A. Nusret BULUTÇU for his laboratory staff for performing the whole experiments.

In addition, I would like to thank my laboratory partners Ece ENGIZEK, Ayşenur ERALP, and Ferhan CİNALİ for contributions to carry out my laboratory studies. I special thanks to Melike ERGUVAN for her friendly atmosphere during the laboratory studies.

Finally, I thank very much to my dear family and close friends, especially Batchimeg DASHDORJ for their motivation, support, helps through the project.

May 2016

Bolormaa BAYARKHUU
(Chemical Engineer)

TABLE OF CONTENTS

	<u>Page</u>
FOREWORD	ix
TABLE OF CONTENTS	xi
LIST OF TABLES	xiii
LIST OF FIGURES	xv
SUMMARY	xvii
ÖZET	xix
1. INTRODUCTION	1
1.1 Background	1
1.2 Outline of Thesis	2
2. LITERATURE REVIEW	3
2.1 Boron and Boron Chemicals	3
2.1.1 Global and Turkish boron reserves	3
2.1.2 Applications of borax and boric acid	5
2.1.3 Demand of borax and boric acid	5
2.1.4 Production processes of borax and boric acid.....	6
2.1.5 Borax and boric acid waste disposal burdens	7
2.2 Theory	9
2.2.1 Physical and chemical properties.....	9
2.2.1.1 Physical and chemical properties of borax.	9
2.2.1.2 Physical and chemical properties of boric acid.....	10
2.2.2 Fundamentals of crystallization process	11
2.2.3 Mechanisms of crystallization process	12
2.2.3.1 Nucleation	12
2.2.3.2 Crystal growth.....	13
2.2.4 Product characteristics	13
2.3 Eutectic Freeze Crystallization (EFC)	14
2.3.1 Definition and separation principle.....	14
2.3.2 EFC process and its advantageous	15
3. MATERIALS AND METHODS	17
3.1 Materials	17
3.2 Experiments	18
3.2.1 1 liter crystallizer set-up.....	18
3.2.2 Experimental procedure	19
3.3 Methods.....	21
3.3.1 Concentration measurement.....	21
3.3.2 Supersaturation	21
3.3.3 Measurement procedure of crystal size.....	21
4. RESULTS AND DISCUSSION	23
4.1 Investigation for Borax-Water ($\text{Na}_2\text{B}_4\text{O}_7\text{-H}_2\text{O}$) System	23
4.2 Investigation for Boric Acid-Water ($\text{H}_3\text{BO}_3\text{-H}_2\text{O}$) System	31
5. CONCLUSIONS	37
6. RECOMMENDATIONS	39
REFERENCES	41

APPENDICES	45
CURRICULUM VITAE	61

LIST OF TABLES

	<u>Page</u>
Table 2.1 : Global boron reserves	4
Table 2.2 : Capacities of boron products from reserve in Turkey.....	5
Table 2.3 : Borate and boric acid solubility in water	9
Table 3.1 : Maximum impurity limits	17
Table 3.2 : Maximum impurity limits	18
Table 4.1 : Crystal size measurement and calculation results.....	29
Table A.1 : Water-Ethylene Glycol concentration and freezing point relations.....	47
Table A.2 : Concentration differences.	48
Table B.1 : Mass and component balance	51

LIST OF FIGURES

	<u>Page</u>
Figure 2.1 : Main borax and boric acid manufacturing plants.....	4
Figure 2.2 : Demand of refined borates between 2014 and 2019	6
Figure 2.3 : Production process of borax	6
Figure 2.4 : Production process of boric acid	7
Figure 2.5 : Kırka plant tailings dam	8
Figure 2.6 : Solubility versus temperature curves for borates and boric acid	10
Figure 2.7 : Solubility diagram showing stable, labile and metastable zones	11
Figure 2.8 : Kinetics in general phase diagram for binary aqueous solutions	14
Figure 2.9 : Schematic representation of EFC process.....	15
Figure 3.1 : Schematic diagram (a) and experimental set-up photo (b).....	20
Figure 3.2 : Automatic titrator (Schott Titronic Universal).....	21
Figure 3.3 : Microscope instrumentation	22
Figure 4.1 : Experimental investigations outline	23
Figure 4.2 : Temperature-Time diagram of borax	24
Figure 4.3 : Concentration-Temperature diagram for borax.....	25
Figure 4.4 : $\text{Na}_2\text{B}_4\text{O}_7 \cdot 10\text{H}_2\text{O}$ salt- ice and $\text{Na}_2\text{B}_4\text{O}_7$ aqueous solution separation	26
Figure 4.5 : $\text{Na}_2\text{B}_4\text{O}_7$ % amounts in solution and ice, after filtration and washing steps	27
Figure 4.6 : (a) $\text{Na}_2\text{B}_4\text{O}_7$ salt, (b) ice crystal images	27
Figure 4.7 : The salt crystal ($\text{Na}_2\text{B}_4\text{O}_7$) captures in the ice	28
Figure 4.8 : Time versus Characteristic Radius Graph for $\Delta T=4.94$ °C	30
Figure 4.9 : Time versus Characteristic Radius Graph for $\Delta T=5.26$ °C	30
Figure 4.10 : Time versus Characteristic Radius Graph for $\Delta T=6.46$ °C.	31
Figure 4.11 : Supersaturation (ΔT)-Growth Rate Graph for $\text{Na}_2\text{B}_4\text{O}_7 \cdot 10\text{H}_2\text{O}$ crystals.....	31
Figure 4.12 : Temperature-Time diagram of boric acid	32
Figure 4.13 : Concentration-Temperature diagram for boric acid.....	33
Figure 4.14 : Boric acid salt-ice and solution at the eutectic point.....	34
Figure 4.15 : H_3BO_3 % amounts in solution and ice after filtration and washing steps	35
Figure 4.16 : (a) H_3BO_3 salt, (b) ice crystal image	35
Figure A.1 : Differences between initial concentration and titration measurements	49
Figure B.1 : Experimental steps before filtration.....	50

EUTECTIC FREEZE CRYSTALLIZATION OF BORON COMPOUNDS

SUMMARY

Boron compounds, especially borax and boric acid, are desired and important raw material in various industries. They have numerous applications from agriculture to nuclear reactors. Major usage of borax and boric acid includes borosilicate glass, ceramic glazes and detergent. Generally, borax and boric acid production is manufactured from tincal and colemanite minerals. Turkey is the world leader of tincal (35.5% B_2O_3) and colemanite (50.8% B_2O_3) minerals. In Turkey, 803 million ton boron reserve exists, and every day several hundred to thousand tons boron waste is discharged in industrial processes.

Before getting environmental awareness and consciousness, those wastes were disposed directly to the environment. Nowadays industrial wastes are enriched to reuse or wastes are discharged in appropriate way due to the negative environmental and ecological impacts. Three major options are available for the management of boron containing wastes:

- recovery of boron minerals from tailings,
- safe disposal of boron tailings without harming the environment,
- utilization of boron tailings as raw materials in ceramics and cement industry.

The continuous demand and consumption of raw materials and water in the world has increased significantly in the past decades. This leads to the necessity for sustainable processes and technologies in the development of raw material and for optimization of processes as regards recycling of wastewater, recovery of waste stream, and energy efficiency. This characterizes the commonly known “Eutectic Freeze Crystallization” (EFC) technology in recent.

This technology is in particular suited for the treatment of aqueous waste streams. The basis of eutectic freeze crystallization is the existence of eutectic point. The eutectic point refers to a characteristic point in the phase diagram of a salt-water mixture. At this temperature an equilibrium exists between ice, salt and a solution with a specific concentration. Thus, eutectic freeze crystallization process converts an invaluable and/or hazardous waste stream into clean water and valuable solid salt products. Besides, EFC has the biggest potential to treat aqueous streams at low cost and high yields.

In this thesis, the primary purpose is to investigate eutectic points of borax-water ($Na_2B_4O_7-H_2O$) and boric acid-water ($H_3BO_3-H_2O$) systems.

The first stream, synthetic borax stream, was used for investigating the eutectic point in a 1 liter EFC experimental set-up. After crystallization process was conducted, ice product purity was detected. In addition, salt crystal size measurement was conducted for evaluating the salt crystal growth at different supersaturation process and different batch times. This aims to calculate the borax growth rates at different supersaturations under EFC conditions. In this experiment, microscopic studies were conducted by using Olympus BX51 microscope.

The second stream, synthetic boric acid stream, was used for investigating the eutectic point in a 1 liter EFC experimental set-up. Similar to borax case, after crystallization process was conducted, the ice product purity was detected.

All experiments were done using starting compositions of 2 wt% borax aqueous, and 2.5 wt% boric acid aqueous solutions. The experimental investigations and feasibility of EFC applications for boron systems were discussed in result and discussion part. Detailed calculation of the processes and additional microscopic images were given in Appendices.

BOR BİRLEŞİKLERİN ÖTEKTİK DONDURMA KRİSTALİZASYONU

ÖZET

Boron birleşikleri, özellikle boraks ve borik asit, çeşitli endüstriler için istenilen önemli hammaddelerdir. Tarımdan nükleer reaktörlere kadar çok sayıda uygulamaları bulunmaktadır. Boraks ve borik asidin ana kullanım alanları borosilikat cam, seramik sır ve deterjan üretimidir. Genel olarak boraks ve borik asit ürünleri, tinkal ve kolemanit minerallerinden üretilmektedir. Türkiye tinkal (35.5% B₂O₃) ve kolemanit (50.8% B₂O₃) kaynaklarıyla dünya lideridir. Türkiye’de 803 milyon ton bor rezervi bulunmakta ve günde tonlarca bor atığı endüstriyel süreçlerde oluşmaktadır.

Bor üretim tesislerinden çıkan atıklar genellikle ince boyutlu katı veya pülp halindedir. Çevre duyarlılığı ve bilinci gelişmeden önce, bu atıklar direkt çevreye atılıyordu. Günümüzde endüstriyel atıklar, yeniden kullanılmak üzere zenginleştirmekte veya kullanılmayan kısımları çevresel ve ekolojik etkilerinden dolayı uygun şekilde imha edilmektedir. Gelişmiş ülkeler başta olmak üzere, Dünya'nın birçok ülkesinde araştırmacılar ve işletmeler bu konuda yoğun çaba harcamaktadır. Başta çevresel ve ekonomik koşullar göz önüne alındığında, bor atıklarının değerlendirilmesi konusunda yeni bir yönteme ihtiyaç duyulmaktadır. Bor içeren atıkların yönetiminde üç temel seçenek mevcuttur:

- bor minerallerinin atıktan geri dönüştürülmesi,
- bor atıklarının çevreye zarar vermeden imha edilmesi,
- bor atıklarının seramik ve inşaat sektöründe hammadde olarak kullanılmasıdır.

Bu durum, sürdürülebilir proses ve teknolojileri, hammadde gelişimi, -atık su geri kazanımı ve enerji verimi gibi- proses optimizasyonlarına yönlendirmiştir. Günümüzde bu amaca “Ötektik Dondurma Kristalizasyon” (ÖDK) teknolojisi hizmet etmektedir.

Bu teknoloji özellikle atık suyunun arıtılması için uygundur. Ötektik dondurma kristalizasyonun temeli ötektik noktanın bulunmasına dayanır. Ötektik nokta, tuz-su karışımı faz diyagramında karakteristik bir noktayı ifade eder. Bu sıcaklıkta buz, tuz ve çözelti arasında belirli bir konsantrasyonda denge oluşmaktadır. Böylece, ötektik dondurma kristalizasyonu prosesi değersiz ve/veya tehlikeli atık çözeltilerini temiz su ve değerli katı tuz ürünlerine dönüştürülmektedir. Ayrıca, ÖDK teknolojisi saf buz ve tuzu son derece düşük maliyet ve yüksek verimde üretmektedir.

Bu tezde, temel amaç boraks-su (Na₂B₄O₇-H₂O) ve borik asit-su (H₃BO₃-H₂O) sistemlerinin ötektik noktalarının araştırılmasıdır.

Birinci atık çözelti, sentetik boraks sistemi, 1 litrelik ÖDK deneysel düzeneğinde ötektik noktanın araştırması için kullanılmıştır. Bu çalışmada, tüm deneyler başlangıçta ağırlıkça 2% boraks sulu çözeltisi kullanılarak yapılmıştır. Karıştırıcı 200 rpm devire ve soğutma makinası -10 °C’ye ayarlanarak kesikli uygulama

süreçlerinde ötektik noktası bulunmuştur. Şekil 4.3'te boraks-su çözünürlük grafiği verilmiştir. Yapılan 11 tane deney sonucunda ötektik nokta 1.06% $\text{Na}_2\text{B}_4\text{O}_7$ ve -0.74 °C olarak tayin edilmiştir.

Ötektik Dondurma Kristalizasyon prosesi uygulandıktan sonra, buz ürün saflığı tespit edilmiştir. Bu çalışmadan elde edilmek istenilen bir diğer veri ise ötektik noktaya ulaştıktan sonra buzun safsızlık içeriğidir. Ötektik noktada, $\Delta T = 6$ °C'lik sürücü güç (soğutucu akışkan -etilen glikol- ve boraks çözeltisi arasındaki sıcak farkı) altında 60 dakika buz ve $\text{Na}_2\text{B}_4\text{O}_7 \cdot 10\text{H}_2\text{O}$ tuz kristallerinin büyümesi ve yoğunluk farkıyla birbirinden ayrılması sağlanmış (Şekil 4.4); ardından süzme ve yıkama işlemleri yapılmıştır. Süzme işlemi cam filtre yardımıyla vakum filtrasyonu ile gerçekleştirilmiştir. Süzülen buz için toplamda iki yıkama gerçekleştirilmiş ve her yıkama sonrası buzun ve alttaki çözeltinin ağırlıkları ölçülerek analiz için numuneler alınmıştır. Her birinden alınan numuneler titrasyon yöntemi ile analiz edilmiş. Sonucu olarak Şekil 4.5'de ötektik noktadaki tuz, buz, çözelti miktarları ve yıkamalar sonucu buzdaki safsızlık gösterilmiştir.

Alınan tüm numuneler Schott Titronic Universal otomatik büret ile analiz edilmiştir. Ötektik noktaya ulaşılmış çözeltiden alınan 10 ml'lik numunenin boraks konsantrasyonu 0.1 N'lık NaOH çözeltisi ile yapılan titrasyonla belirlenmektedir.

Ayrıca farklı ÖDK koşullarında süper-doygunluk ve değişik kesikli uygulama süreçlerinde (10 dakika, 30 dakika, 1 saat ve 5 saat), tuz kristal boyutunun ölçümü yapılmış ve büyüme hızı araştırılmıştır. Bu deneysel çalışmada, tuz ve buz kristalleri boyut ve görünüm özellikleri açısından Olympus BX51 marka mikroskop altında incelenmiştir. Mikroskop ile gözlemlenen kristallerin fotoğrafları optik mikroskopun 5X büyütme özelliği ile çekilmiş ve Image-Pro Plus programı yardımıyla boyutlandırılmıştır.

Deney sonrası, tuz kristalinin kaydedilen görüntüleri, Image J programı yardımıyla boyutlandırılmış ve meydana gelen değişimler hesaplanmıştır.

Deneysel sonuçlar kısmında, boraks kristallerinin büyüme hızı ΔT ile değişimi grafiği ile ifade edilmiş ve Şekil 4.11'te gösterilmiştir. Sonucu olarak 3×10^{-9} m/s bulunmuştur.

İkinci atık çözelti, sentetik borik asit sistemi, 1 litrelik ÖDK deneysel düzeneğinde ötektik noktanın araştırması için kullanılmıştır. Bu çalışmada, tüm deneyler başlangıçta ağırlıkça 2.5% borik asit sulu çözeltisi kullanılarak yapılmıştır. Karıştırıcı 200 rpm devire ve soğutma makinası -10 °C'ye ayarlanarak kesikli uygulama süreçlerinde ötektik noktası bulunmuştur. Şekil 4.3'te boraks-su çözünürlük grafiği verilmiştir. Ötektik nokta 2.57% H_3BO_3 ve -0.75 °C olarak tayin edilmiştir.

Ötektik Dondurma kristalizasyon prosesi uygulandıktan sonra, borakstaki gibi buz ürün saflığı tespit edilmiş ve sonucu Şekil 4.5'de gösterilmiştir. Ötektik noktada, $\Delta T = 4$ °C'lik sürücü güç altında 20 dakika büyümesi sağlanmış, ve H_3BO_3 tuz kristallerinin yoğunluk farkıyla birbirinden ayrılması sağlanmıştır (Şekil 4.14).

Tuz ve buz kristalleri bir cam filtre yardımıyla vakum filtrasyonu yapılarak ayırmıştır. Daha sonra alınan çözelti numunesinin analizi aynı şekilde titrasyon ile yapılarak tuz, buz, çözelti miktarları ve yıkamalar sonucu buzdaki konsantrasyon belirtilmişti (Şekil 4.15).

Bu deneysel çalışmada, tuz ve buz kristalleri boyut ve görünüm özellikleri açısından da Olympus BX51 marka mikroskop altında incelenmiştir. Mikroskop ile gözlemlenen kristallerin fotoğrafları optik mikroskopun 5X büyütme özelliğinde çekilmiştir.

Ayrıca vakum filtrasyonu yapılarak tuz ve buz ayrıldıktan sonra kütle dengesi kurularak ötektik noktadaki tuz, buz, çözelti miktarları ve yıkamalar sonucu dengesini sağlatmıştır. Detaylı hesaplama Ek B’de gösterilmiştir.

Bor içeren çözeltilerde deneysel arařtırmalar ve ÖDK uygulama fizibilitesi, sonuç ve tartışmalar kısmında ele alınmıştır. Prosesin ayrıntılı hesabı ve mikroskobik görüntüleri Ekler kısmında verilmiştir.

1. INTRODUCTION

1.1 Background

Boron is the 51st most common element and occurs in borates and borosilicate in the earth's crust [1]. Boron minerals are located in eight different countries all around the world and 72% of known boron reserves are found in Turkey. Boron and its compounds have a wide field of applications including glass products, cleaning products, flame proofing and corrosion [2].

With development of technology, the areas where boron is used are increasing. It becomes obvious that the total boron compound demand in the industry is growing each year. The manufacturing of boron products results in significant amount of different types of boron wastes [3]. At present, these waste streams are discharged in tailings dams. However, this raises substantial environmental concern in fear of leaching, and thus groundwater and soil pollutions. In order to address these problems, many processes have been suggested concerning boron waste utilization. For recovering boron waste, the potential way is to use them as an additive material in clay mixtures for the production of ceramics and cements [3-5].

Environmental protection and energy saving are considered to be crucial matters in industries. Therefore, in addition to finding alternative raw materials, recycling wastes as possible replacement has gained considerable interest within last years [5]. 'Nearly Zero Liquid Discharge (ZLD)' concept has recently been investigated by various groups, and was the focus of several reviews [6-9]. Nowadays, one alternative for treating waste/process streams and recovering raw materials and water aiming to reach ZLD is achieved by using Eutectic Freeze Crystallization technology [10].

In this thesis we apply novel Eutectic Freeze Crystallization (EFC) technology to treat boron containing waste streams. For this particular study, borax and boric acid solutions were chosen. The following actions were investigated in the context of this study.

- Eutectic temperatures and compositions (i.e. eutectic points) of borax-water and boric acid-water systems were detected,
- Qualities and purities of recovered ice (water) were investigated both for eutectic borax and eutectic boric acid systems,
- Salt crystal growth for borax crystals were investigated at different supersaturations and different batch times.

1.2 Outline of Thesis

EFC is a recently developed technology to treat aqueous solutions from chemical and metallurgical industries. This thesis focuses on the feasibility of EFC on the treatment of borax and boric minerals in batch operation.

Chapter 2 provides an overview based on literature review: boron chemicals, borax and boric acid industrial production processes, main applications and demands of borax and boric acid. Moreover, definition of Eutectic Freeze Crystallization process and its advantageous is presented in this chapter. In addition, basics of crystallization phenomena is discussed.

Chapter 3 focuses on the materials used in experimental operation and detailed experimental set-up and methods used for investigations of this thesis.

Chapter 4 covers the discussions on results of experiments, and Chapter 5 carries the conclusion, respectively.

2. LITERATURE REVIEW

2.1 Boron and Boron Chemicals

Boron, chemical symbol B and atomic number 5, is the only non-metallic Group III A element in the periodic table. It was discovered by British chemist Sir Humphry Davy and independently French chemists Joseph Gay-Lussac and Louis Thenard in 1808 [11].

Boron is a widely occurring element and estimated to constitute approximately 0.001% of the earth's crust [12]. Besides, the boron content occurs in fresh water, seawater, soil and rocks. Although it is widespread in nature, the presence of boron occurs only in very small amounts in nature [13] and boron does not occur in nature as a free element. There are more than 230 naturally occurring boron containing minerals in all around World [14]. The most commercially important minerals are borax decahydrate ($\text{Na}_2\text{B}_4\text{O}_7 \cdot 10\text{H}_2\text{O}$), boric acid (H_3BO_3), kernite ($\text{Na}_2\text{B}_4\text{O}_7 \cdot 4\text{H}_2\text{O}$), colemanite ($\text{Ca}_2\text{B}_6\text{O}_{11} \cdot 5\text{H}_2\text{O}$) and ulexite ($\text{NaCaB}_5\text{O}_9 \cdot 8\text{H}_2\text{O}$) which are considered as minerals that provide the source for the world's production [15].

2.1.1 Global and Turkish boron reserves

The main reserves of boron minerals in the World are available in Turkey and USA. Further mining and production facilities exist in Argentina, Bolivia, China, Chile, Peru, and Russia [16]. Around 25% of global boron production, mainly in the form of borax and kernite was produced from Boron Mine in USA in 2012, whereas 72% of global boron production was manufactured from Eti Mine in Turkey. The balance of production was dominated from China, Argentina and Chile [17]. In Table 2.1, global boron reserves are shown as boric oxide (B_2O_3) [18].

Table 2.1 : Global boron reserves.

Location	Total reserve (B₂O₃ thousand tons)	(%)
Turkey	955.300	72.8
USA	80.000	6.1
Russia	100.000	7.6
China	47.000	3.6
Argentina	9.000	0.7
Bolivia	19.000	1.4
Chile	41.000	3.2
Peru	22.000	1.7
Kazakhstan	15.000	1.2
Serbia	24.000	1.7
TOTAL	1.312.300	100

Turkish boron deposits are located in western side at five main districts: Bigadiç, Sultançayır, Kestelek, Emet and Kırka [19]. In order to utilize mining resources more effectively, boron operation in Turkey was transferred to Eti Mine in 1935. The high added value products of boron such as borax decahydrate, borax pentahydrate, boric acid, and boric oxides are produced in Eti Mines and most of them are exported. According to Eti Mine, total capacity for boron products are 2.13 million tons/year. Boron products manufactured in Turkey by Eti Mine are listed in Table 2.2 [18]. Eti Bor operates plants at Emet (capacity 100.000 tons/year), Bandırma (capacity 85.000 tons/year), and Kırka (840.000 tons/year) (Figure 2.1) that produce main borax and boric acid products in Turkey [20].



Emet plant



Bandırma plant



Kırka plant

Figure 2.1 : Main borax and boric acid manufacturing plants [20].

Table 2.2 : Capacities of boron products from reserve in Turkey [18].

Products	Thousand tons/year
Borax decahydrate (Bandırma)	115
Boric acid (Bandırma)	95
Anhydrous borax	5
Sodium perborate (Bandırma)	35
Boron oxide (Bandırma)	2
Boric acid (Emet)	240
Borax pentahydrate (Kırka)	840
Borax decahydrate (Kırka)	80
Colemanite (Bigadiç)	700
Calcined tincal (Kırka)	5
Agriculture Boron (Bandırma)	8
Glassy Boron Oxide (Bandırma)	6
TOTAL	2.131

2.1.2 Applications of borax and boric acid

Borax and boric acid are essential raw materials with great potential in various applications. Borax has a wide application and used in areas such as borosilicate glasses, glass wool, ceramics, detergents, cement and fire proof materials [2]. Borax is also frequently used to provide corrosion inhibition for ferrous metals and traditionally used in steel and stainless steel wire in metallurgical industry [11], [21].

Boric acid is also a crucial raw material for several industries. It is one of the important component for fiber-glass and borosilicate glass production, which is a heat-resistant product also named as Pyrex. Pyrex has wide uses such as laboratory equipment, cookware, TV screen, computer monitors (CRT and LCD) as well as in a wide range of optical instruments from microscope slides to observatory mirrors [11], [21].

2.1.3 Demand of borax and boric acid

Due to increasing economies and industries, the demand for boron products are expected to grow. Growing population is the driving force for borates demand in

urbanization, food supply and energy. This demand is expected to increase continuously as shown in Figure 2.2 [22].

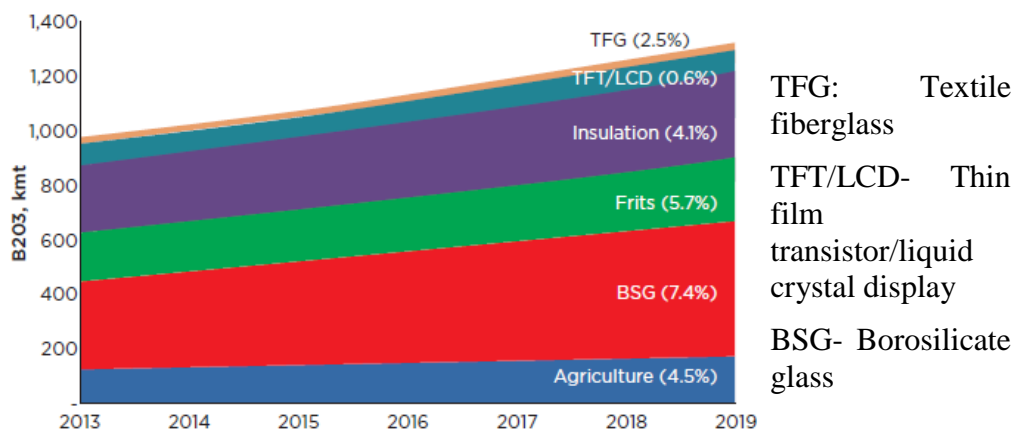


Figure 2.2 : Demand of refined borates between 2014 and 2019 [22].

2.1.4 Production process of borax and boric acid

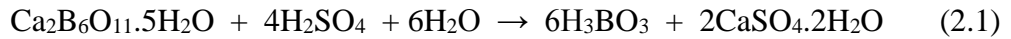
Boron ores are used in production of various boron derivatives. Colemanite and tincal are crucial ores for production of borax and boric acid.

Borax: Borax is generally prepared from the tincal ore which is dried from lakes. The production of borax process is proceeded by dissolving, precipitation, filtration, crystallization and drying as shown in Figure 2.3. Borax decahydrate product can be obtained with a minimum 36.5% B₂O₃ grade [23].



Figure 2.3 : Production process of borax [18].

Boric acid: Boric acid is generally produced from colemanite or tincal reacting with H_2SO_4 . The production process of boric acid from concentrated colemanite is proceeded by crushing, grinding, reaction with sulfuric acid, filtration, and crystallization. In Figure 2.4, production processes of boric acid is demonstrated [18]. Boric acid product can be obtained with a minimum 56% B_2O_3 grade. The reaction is shown in equation 2.1 [24].



As reported in literature, boric acid is produced from tincal concentrate by several methods. One of them is dissolving tincal concentrate with nitric acid or hydrochloric acid. Another method is electrolysis of aqueous tincal concentrate at 80 °C. In general, boric acid is produced with sulfuric acid from tincal. In this production of boric acid is conducted with the reaction shown in equation 2.2 [24].

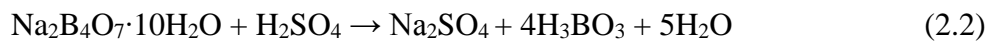


Figure 2.4 : Production process of boric acid [18].

2.1.5 Borax and boric acid waste disposal burdens

Mining operation for obtaining of boron products is open pit, and underground processes. Concentrations of boron minerals are either directly marketed or treated to produce refined products as a borax decahydrate, pentahydrate, perborate, and boric acid [4].

Over 1.5 million tons of boron products were produced in 2001 in all around the World. Turkey and USA share about 33.4% and 42% of total boron production, respectively. Ediz and Özdemir stated that during the production processes in Turkey annually almost 600.000 tons of boron wastes, and particularly only in tincal plants approximately 400.000 tons of borax wastes are generated [25], [26]. Conventional disposal way of aqueous boron wastes is to store in tailings dams. However, it is not sustainable. The largest borax processing plant, Kırka, where tailings are pumped to 13.000.000 m³ capacity tailings ponds that are almost filled up. The shortage of waste ponds (Figure 2.5) creates a serious problems including occupation of large areas of land and environmental pollutions. It is known that the tailings ponds contain around 12.000.000 m³ of materials of which 6.500.000 m³ is waste water containing boron. Another fatal problem faced in storing boron waste in tailing pond is storing wastes in leakage free ponds. Although boron is necessary compound for living organism and the habitat, higher concentrations of boron become environmentally hazardous [27].



Figure 2.5 : Kırka tailings dam [28].

Thus, the most suitable strategy appears to be the recovery of boron tailings followed by its industrial utilization. The recycling boron wastes are intended to provide the following benefits [25]:

- Environmental pollution will be reduced,
- Waste storing problems and storing costs will be reduced,
- Groundwater and surface water contaminants will be prevented,
- Additional boron waste based products will be produced.

Due to environmental issues related to industrial waste, recovery of salts and water from those waste streams is an essential matter. It is expected in 2007 by the United

Nations that, water consumption of the World will increase very steep in the coming 20 years up to $6 \times 10^6 \text{ m}^3$ [29]. Using the waste streams, the recovered water can be used as process water; and the crystallized salt can be a commercial product. In other words, these streams could easily be turned into valuable products once an affordable treatment technology is available. The new waste-to-products paradigm which treats waste streams as raw materials is environmentally crucial for recycling and protecting the world's natural resources, and also economically favorable by decreasing the production cost [30].

In this study, for treatment of boric acid-water and borax-water systems, the novel Eutectic Freeze Crystallization technology is applied.

2.2 Theory

2.2.1 Physical and chemical properties

2.2.1.1 Physical and chemical properties for borax

Borax or borax decahydrate, $\text{Na}_2\text{B}_4\text{O}_7 \cdot 10\text{H}_2\text{O}$ or $\text{Na}_2\text{O} \cdot 2\text{B}_2\text{O}_3 \cdot 10\text{H}_2\text{O}$, is most known name of the disodium tetraborate decahydrate. Borax decahydrate is odorless, white, monoclinic prisms with density 1.711-1.715 g/cm^3 . The molecular weight of borax is 381.36 g/mol and its specific heat is 1.611 $\text{kJ}/(\text{kg K})$ at 25-50 $^\circ\text{C}$ as well as a heat of formation is -6.264 MJ/mol . It crystallizes from aqueous solution below 60.8 $^\circ\text{C}$. The solubility-temperature curves for the $\text{Na}_2\text{O} \cdot 2\text{B}_2\text{O}_3 \cdot 10\text{H}_2\text{O}$ system and solubility of borax solution are given in Table 2.3 and Figure 2.6, respectively [31], [32].

Table 2.3 : Borate and boric acid solubility in water [1].

Compound	Solubility in wt% anhydrous salt at T ($^\circ\text{C}$)										
	0	10	20	30	40	50	60	70	80	90	100
$\text{NaBO}_2 \cdot 4\text{H}_2\text{O}$	14.5	17	20	23.6	27.9	34.1					
$\text{NaBO}_2 \cdot 2\text{H}_2\text{O}$							38.3	40.9	43.7	47.4	52.4
$\text{Na}_2\text{B}_4\text{O}_7 \cdot 10\text{H}_2\text{O}$	1.0	1.6	2.5	3.8	5.9	9.5	16.0				
$\text{Na}_2\text{B}_4\text{O}_7 \cdot 5\text{H}_2\text{O}$							16.4	19.5	23.4	28.1	34.6
$\text{Na}_2\text{B}_4\text{O}_7 \cdot 4\text{H}_2\text{O}$						14.2	14.7	17.0	19.7	23.0	27.2
$\text{B}(\text{OH})_3$	2.4	3.5	4.7	6.2	8.8	10.3	13.0	15.8	19.1	23.3	27.5

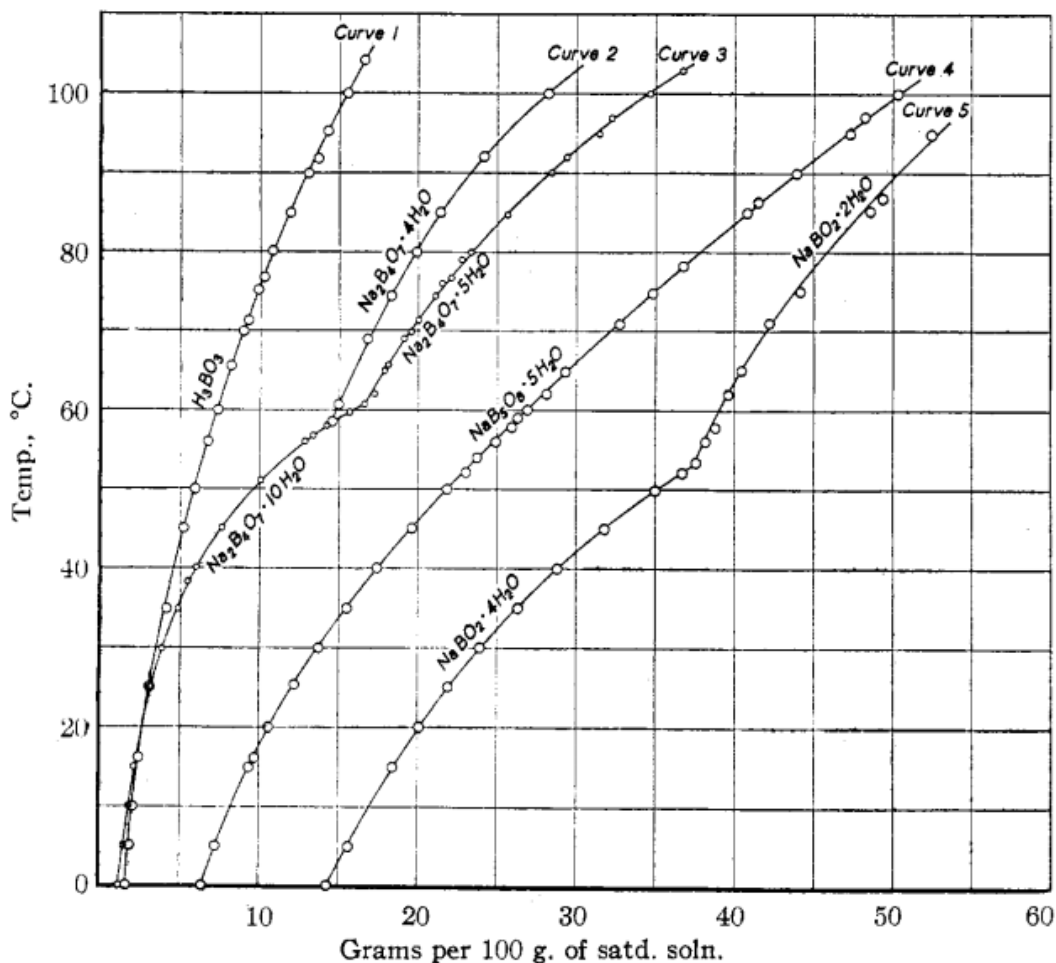


Figure 2.6 : Solubility versus temperature curves for borates and boric acid [32].

2.2.1.2 Physical and chemical properties for boric acid

Boric acid, H_3BO_3 ($\text{B}_2\text{O}_3 \cdot 3\text{H}_2\text{O}$), exist as the trihydrate, and orthoboric acid. Orthoboric acid is referred as boric acid in general. Boric acid, $\text{B}(\text{OH})_3$, crystallizes from aqueous solutions and appearance of the acid is white, waxy platelets with a density of 1.51 g/cm^3 (20°C). The weight of boric acid is 61.83 g/mol , and its heat of formation is -1089 kJ/mol [1].

The boric acid acts as a weak acid in aqueous solutions and its acidity rise with temperature. Solubility data in water is shown in Table 2.3 and solubility curve illustrated in Figure 2.6. Solubility of boric acid in water is increased by adding salts such KCl , KNO_3 , RbCl , K_2SO_4 and NaSO_4 , whereas addition of LiCl , NaCl , and CaCl_2 decrease its solubility [31].

2.2.2 Fundamentals of crystallization process

Crystallization is a common unit operation which is used for purification, separation, production step, yielding quality crystals in chemical industry. Crystallization has become a technique in wide range areas such as biotechnology, mineral processing, waste treatment, pollution abatement, energy storage, new construction materials, and electronic chemicals. The process is applied as a separation technique in inorganic chemical industry in order to recover salts from aqueous solutions [33].

Supersaturation in a solution is the driving force of the crystallization processes. Level of supersaturation is an important factor for nucleation and growth of the crystal. Supersaturation can be achieved by different ways. Most commonly used method is cooling the solution. This is preferred when the solubility of solute is sharply dependent on temperature [34]. Another widely applied method in order to generate the supersaturation is evaporation. The method is mostly used when the solubility slightly relies on temperature. By adding an extra substance, supersaturation can also be created in a solution [35].

As described in Figure 2.7, there are two important curves, namely solubility (saturation) and nucleation (supersaturation) curves and three main regions, including stable (unsaturated), metastable and labile (saturated) zones [36].

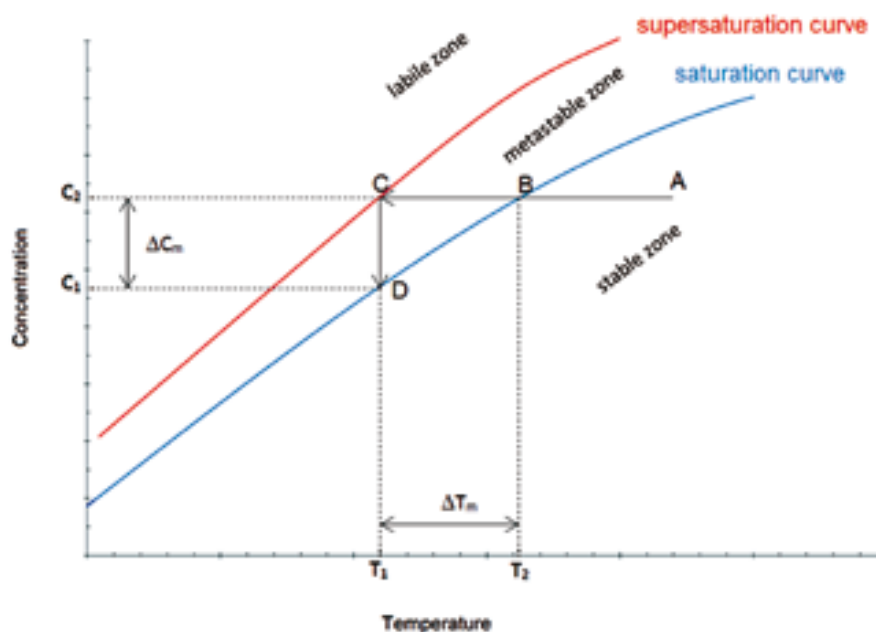


Figure 2.7 : Solubility diagram showing stable, labile and metastable zones [36].

- Lable or unstable zone is the saturated region where nuclei grow spontaneously.
- Metastable zone is the important region among these three zones and is a supersaturated region where crystals grow. The thickness of this region is said metastable zone width. The metastable zone width is measured by determining the point at which first crystal nuclei are detectable. This can be achieved by several ways, such as optical methods, including turbidity measurements or ATR-FTIR (attenuated total reflectance Fourier transform infrared spectroscopy), by calorimetry and image analysis. And information based on the metastable zone width is used for estimation for nucleation kinetics.
- Unsaturated or stable zone is the undersaturated region where crystals dissolve [37].

2.2.3 Mechanisms of crystallization process

2.2.3.1 Nucleation

Nucleation is the formation of embryos/seeds in a supersaturated solution. Nucleation can be classified into primary nucleation and secondary nucleation. Primary nucleation does not involve crystals in the solution, whereas secondary nucleation includes the crystal of solute or crystals are intentionally added to the solution. Primary nucleation is further divided into homogeneous nucleation and heterogeneous nucleation [38].

Homogeneous nucleation occurs in the absence of foreign particles, and it can be proceeded away from interface like crystallizer wall or impeller as well as impurities. Heterogeneous nucleation occurs by inducing foreign particles; thus, in practice, primary heterogeneous nucleation is encountered in common [38].

Secondary nucleation can occur in presence of crystals of the materials being crystallized. And another possibility of the secondary nucleation causes mostly by collisions with crystallizer, impeller and mixer [33]. This nucleation is divided into three main categories in which apparent, true and contact nucleation. Apparent nucleation refers to a small fragments washed from the surface of seeds when they are introduced into crystallizer. True nucleation occurs simply due to the presence of

the solute particles in solution. Contact nucleation occurs when the growing crystals contact with wall, impeller, or other particles which can produce new nuclei [38].

2.2.3.2 Crystal growth

Once stable nuclei are formed, nuclei begin to grow into visible size, this process is crystal growth [38].

The mechanism of crystal growth from a solution requires the solute to be transported on to the crystal surface and then oriented into the crystal lattice. The rate of crystal growth is the mechanism which is expressed with following equation [33]:

$$G=dL/dt \quad (2.3)$$

Where L is characteristic length.

Crystal growth is a two-step mechanism: (i) diffusion in which mass transfer of solute molecules from solution to the crystal surface by diffusion and (ii) surface reaction in which incorporation of the material into the crystal lattice through surface adsorption [34].

The solute molecules reach the growing faces of the crystal by diffusion from the bulk of the liquid phase. When the solute molecules orient themselves into crystal lattice by reaction, there three different attachment exit such as kinks, ledges and terraces attachments on crystal surfaces. The attachment at kinks is the most favorable and followed by the attachment at ledges and the attachment at terraces [34].

2.2.4 Product characteristics length

The main characteristics of a salt product is its crystal size, shape and purity. Only crystal size was considered in this work and brief descriptions is given in following section.

The crystal size distribution is influenced on many aspects of crystal processing and properties, including appearance, solid-separation, purity, reactions, and other properties. The dominant properties of a product is usually defined by the average crystal size and the width distribution. For batch operation, defining a characteristic length for an operation is a bit tricky since with the batch time change, supersaturation variates [34]. In our calculation for each batch time, supersaturation

is measured and an arithmetic mean crystal size was defined. The details of this procedure will be elaborated in the next section.

2.3 Eutectic Freeze Crystallization (EFC)

2.3.1 Definition and separation principle

Crystallization is a recovery process for a dissolved compound forming a crystalline phase. This process is closely associated with the thermodynamics of the system expressed by the phase diagram, which represent the stable state of the solid and liquid phases in the range of temperature, pressure and composition [41].

Figure 2.8 shows the solubility for a binary phase diagram for a eutectic system. Each point of the solubility lines represents the temperature and the concentration where the solid is in equilibrium with the solution. Eutectic point is the intersection of the ice and salt equilibrium lines (point E). The composition of the feed solution can be at either side of the eutectic point. Eutectic freeze crystallization is the combination of cooling and freeze crystallization [42].

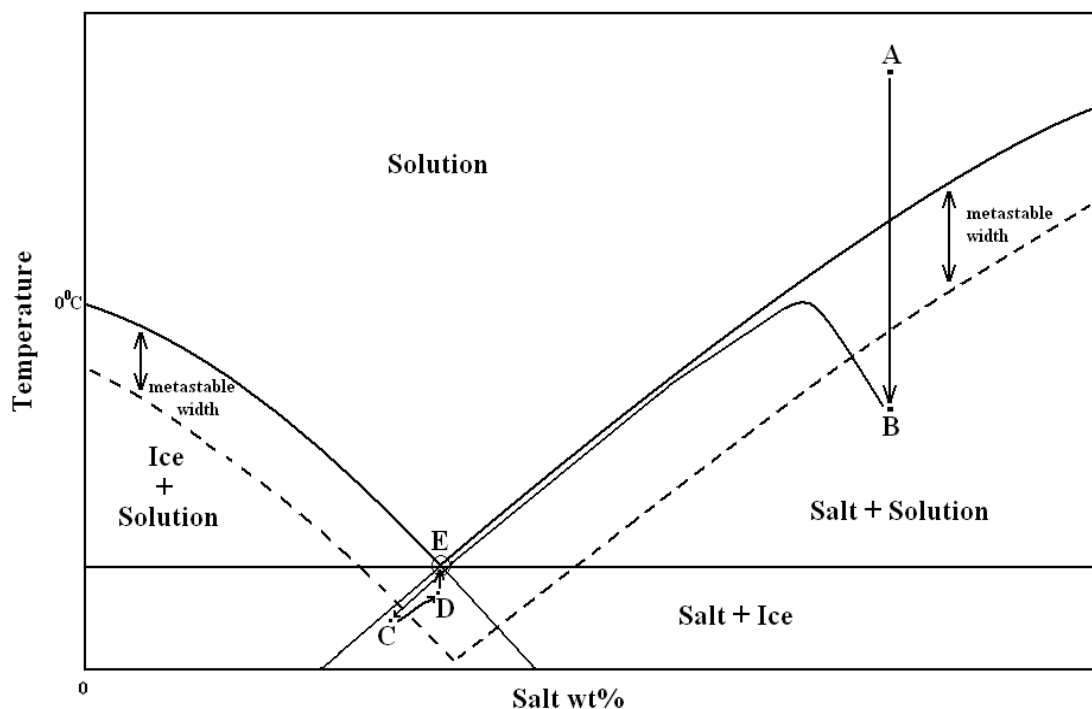


Figure 2.8 : General phase diagram for binary aqueous solutions [42].

Starting for example with a crystal free solution of composition A in a batch process, cooling first leads to the crystallization of the salt. Upon crossing the solubility line,

the solution becomes supersaturated. Within the metastable zone width no nucleation and growth of crystals into measurable sizes will occur within a pre-set time period and only beyond this region the crystallization of the salt noticeable sets in at e.g. point B. The temperature then increases because of the release of heat of crystallization, and the salt concentration in solution decreases. The operational conditions remain close to the solubility line until the metastable region for ice formation is crossed, and ice starts to form at point C. Ice and salt are then produced at supersaturated conditions D just below the eutectic point E, and if we let the system of ice, salt and solution equilibrate at the end of the solution composition will go to point E. For a continuous process the operating conditions within the crystallizer are those reflected by point D for a feed of composition and temperature given by point A. For a feed with a crystal free composition at the left side of the eutectic point first ice will be formed in a batch process, and then a mixture of ice and salt [42].

2.3.2 EFC process and its advantageous

The basic representation of the continuous EFC process is described in Figure 2.9. The process is generally consisted of four unit operations: ice and salt crystallization; separation of the ice and salt, pure water delivery and salt crystals delivery. Ice and salt nucleate and grow in the crystallizer at eutectic point. Ice and salt are then separated due to their density difference in the solid/solid separator from which ice reaches to the wash column (or belt filter) and salt is sent to another belt filter. Pure water and solid salt are the products of EFC process. Eventually, mother liquor (recycled brine) is sent into the crystallizer [43].

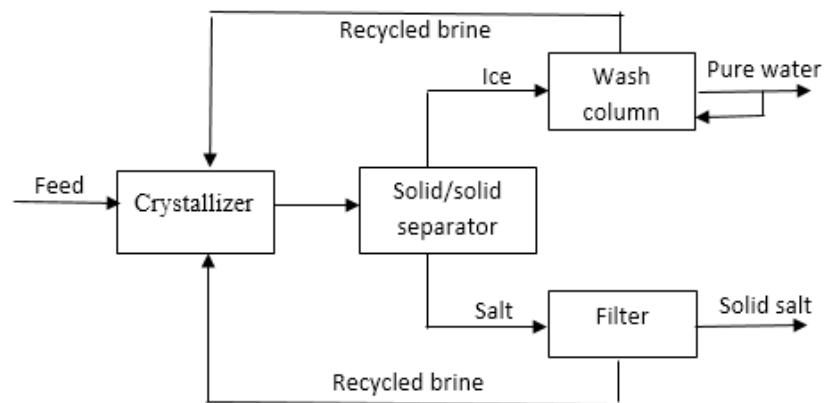


Figure 2.9 : Schematic representation of EFC process [43].

Eutectic Freeze Crystallization [10], [39], [40], [41], [42] is a strong future technology candidate for separation of the dissolved salts and process water from industrial or waste streams. EFC, offers a technologically and economically attractive alternative to conventional separation techniques by recovering pure salt and water product from process or waste streams, thus saving energy or turning waste into raw materials in an energetically favorable way. Besides, EFC is an entirely new type of unit operation which allows completely new, more efficient flow sheets to be designed. EFC operates around the eutectic temperature of aqueous solutions and can treat a wide variety of feed solutions without adding any further solvents or chemicals. EFC is complementary to reverse osmosis for concentrated streams and dissolved inorganic and organic mixtures. With a theoretical yield of 100% and an energy cost saving of up to 90% compared to evaporative crystallization, EFC delivers two products simultaneously: pure salt and pure ice crystals. Separating those products is easily accomplished on account of their density differences [30].

3. MATERIAL AND METHODS

3.1 Materials

Experiments were conducted for two different aqueous solutions; borax solution and boric acid solution. Although the opportunity of treating industrial borax and boric acid solutions are aimed, as a start synthetic solutions were prepared and EFC experiments were performed.

- Borax decahydrate ($\text{Na}_2\text{B}_4\text{O}_7 \cdot 10\text{H}_2\text{O}$) (Merck, impurity content is given in Table 3.1) was used to prepare 2 wt% $\text{Na}_2\text{B}_4\text{O}_7$ aqueous solution for determination of the eutectic point of borax-water system. Same starting borax solution composition was used for crystal growth experiments.

Table 3.1: Maximum impurity limits [45].

Impurity	% Composition
Undissolved compound	0.003
Ammonium (NH_4)	0.001
Carbonate (CO_3)	0.05
Chlorine (Cl)	0.0005
Phosphate (PO_4)	0.001
Sulphate (SO_4)	0.0025
Arsenic (As)	0.0002
Calcium (Ca)	0.005
Heavy Metals (Pb)	0.002
Magnesium (Mg)	0.002
Iron (Fe)	0.0005

- Boric acid, H_3BO_3 , (Merck, impurity content is given in Table 3.2) was used to prepare 2.5 wt% H_3BO_3 aqueous solution for determination of the eutectic point of boric acid-water system.

Table 3.2: Maximum impurity limits [45].

Impurity	% Composition
Undissolved compound	0.003
Ammonium (NH ₄)	0.001
Carbonate (CO ₃)	0.05
Chlorine (Cl)	0.0005
Phosphate (PO ₄)	0.001
Sulphate (SO ₄)	0.0025
Arsenic (As)	0.0002
Calcium (Ca)	0.005
Heavy Metals (Pb)	0.002
Magnesium (Mg)	0.002
Iron (Fe)	0.0005

- Ethylene glycol was used as an indirect coolant in experiments due to its low freezing point. Appendix Table.A1 illustrates the freezing points dependence on water-ethylene glycol concentrations [43]. In this thesis, 40% volumetric ethylene glycol solution was used having a freezing point of -23.3 °C.
- In all experiments de-ionized water with a conductivity of 0.067 µs/cm was used.

3.2 Experiments

3.2.1 1 liter crystallizer set-up

A schematic diagram of the experimental setup is shown in Figure 3.1. The EFC experiments were performed in a 1 liter plastic beaker. The crystallizer was placed in a double walled glass vessel and was cooled indirectly with ethylene glycol solution between the crystallizer and the double walled vessel described in Figure 3.1. An ethylene glycol solution was cooled with a Julabo circulator FP40 cooling machine with a 2.3 kW heating capacity at a range of temperature -40 °C and 200 °C. The temperature was measured with two temperature sensors (T1 and T2) and recorded in a computer. The temperatures were sampled and recorded in a 10 seconds interval with an Agilent multimeter (model LXI 349772A) connected to Temo-Control thermistors (model NTC-8315) with an accuracy of ± 0.01 °C and resistances at 0 °C as 32.7 k Ω [44]. The first sensor (T1) was immersed in the solution and second one (T2) was immersed in the coolant between the crystallizer and the double walled

vessel. In this experiment, Ika Rw 20 agitator -working with 220 V, 50Hz- was used to stir the solution in a range of 60-2000 rpm.

3.2.2 Experimental procedure

The crystallizer was filled with 1 liter of 2 wt% borax solution (or 2.5 wt% boric acid solution). The agitator was started at 200 rpm. Cooling machine was started with a temperature set point of -10 °C. Predictions from Seidell's solubility data [45] indicated approximately 6-7 °C below the eutectic points of borax and boric-acid aqueous solutions. When crystallization of ice and salt had occurred and after crystals have appropriate time for growing (this time varies in each experiment), the stirrer was stopped. The salt crystals were settled at the bottom of the crystallizer and ice crystals were floated at the top due to their density differences. Salt and ice were separated by vacuum filtration over a glass filter. The ice crystal was washed twice with 50 ml pure water which was pre-cooled till 0 °C. The crystallization process was followed by analyzing ice and salt samples from crystallizer under the microscope and by measuring the solution concentration by titration. All experiments were followed by the same procedure.

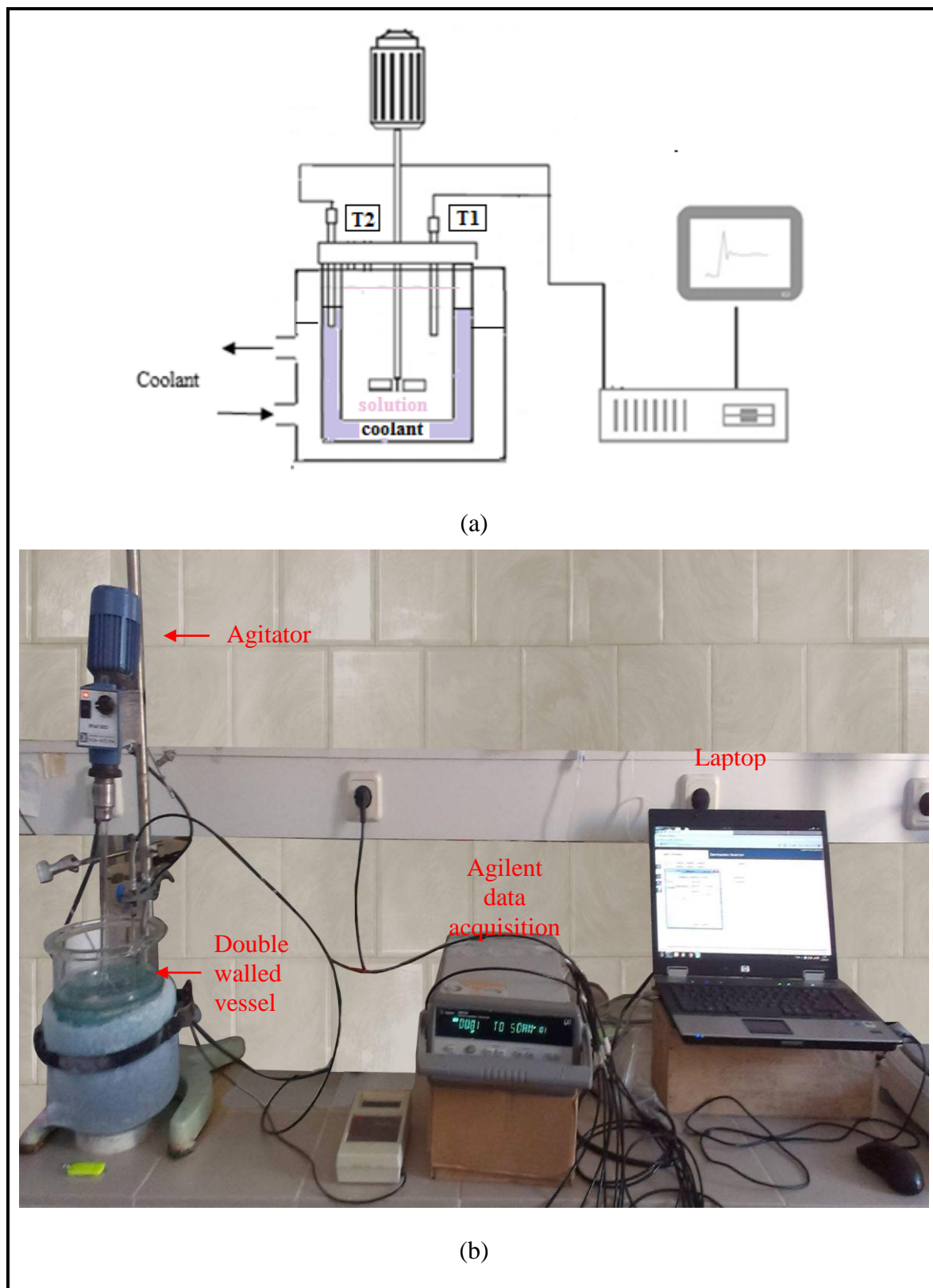


Figure 3.1: (a) Schematic diagram (b) Experimental set-up photo

3.3 Methods

3.3.1 Concentration measurement

Solubility (or phase) diagram is a function of both temperature and concentration. Therefore for defining the state of the solution at a particular temperature on a phase diagram, concentration value has to be measured.

One of the common ways to measure the concentration of the solution is titration method. In our experiments, the concentration of samples were measured with the automatic titrator (Schott Titronic Universal) as illustrated in Figure 3.2. In titration method, 10 mL solution sample was filtered and used to determine the concentration. Using 0.1 N NaOH, titration was conducted [48]. The details of titration method is elaborated in Appendix A.



Figure 3.2 : Automatic titrator (Schott Titronic Universal).

3.3.2 Supersaturation

Supersaturations is the driving force of the system. For our system, we defined it by the temperature difference between the coolant and the bulk temperature within the beaker ($\Delta T_{\text{sup.sat}} = T_{\text{bulk}} - T_{\text{coolant}}$). Due to fact that size, shape and solid state of product crystals depends on supersaturation profile, crystal size distribution is measured under the control of supersaturation.

3.3.3 Measurement procedure of crystal size

After crystallization, crystal sample was taken directly from the crystallizer to the lamella promptly for crystal size measurement. Solution sample was filtered and its

concentration was measured via titration. In each experiment, temperature of solution was recorded during sampling and crystal size measurement. The size of salt crystals was studied with the Olympus BX51 microscope (Figure 3.3). Photographs of salt crystals were taken by objective of optical microscope with 5X magnification and collected with Image-Pro Plus software in computer. By Image Pro Plus, all microscopic photos were visualized and using Image J software area of the crystals were measured [46]. The size parameter is usually estimated as the circle equivalent diameter estimated from measured area, diameter of a sphere of the same volume or from the mass of the crystal using shape factors and density [40]. In this work assuming the crystal shape to be a circle, the circle radius was calculated and by averaging all the radiuses per measurement, a representative crystal size was found. The details of this calculation is presented in results and discussion part.

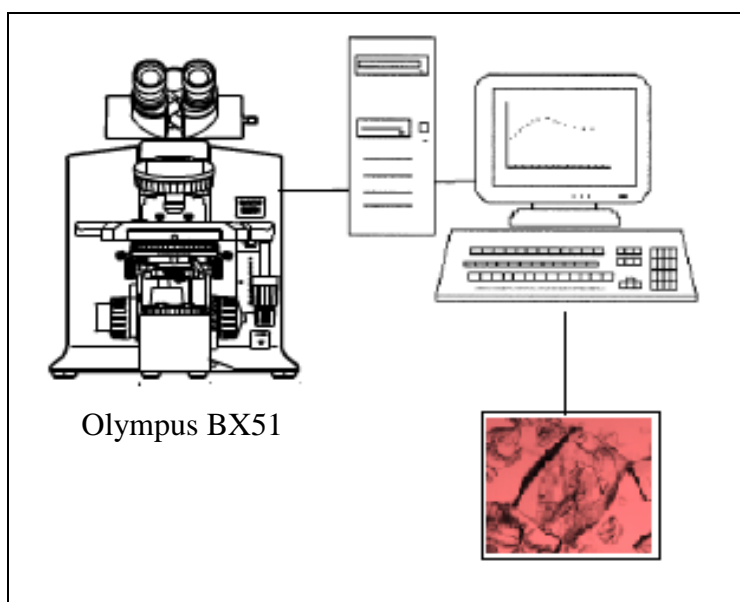


Figure 3.3 : Microscope instrumentation.

3. RESULTS AND DISCUSSION

In this section results of the experiments are presented. Two different aqueous solutions, i.e. borax-water ($\text{Na}_2\text{B}_4\text{O}_7\text{-H}_2\text{O}$) and boric acid-water ($\text{H}_3\text{BO}_3\text{-H}_2\text{O}$) systems were employed. The outline of the experimental investigations are presented in Figure 4.1.

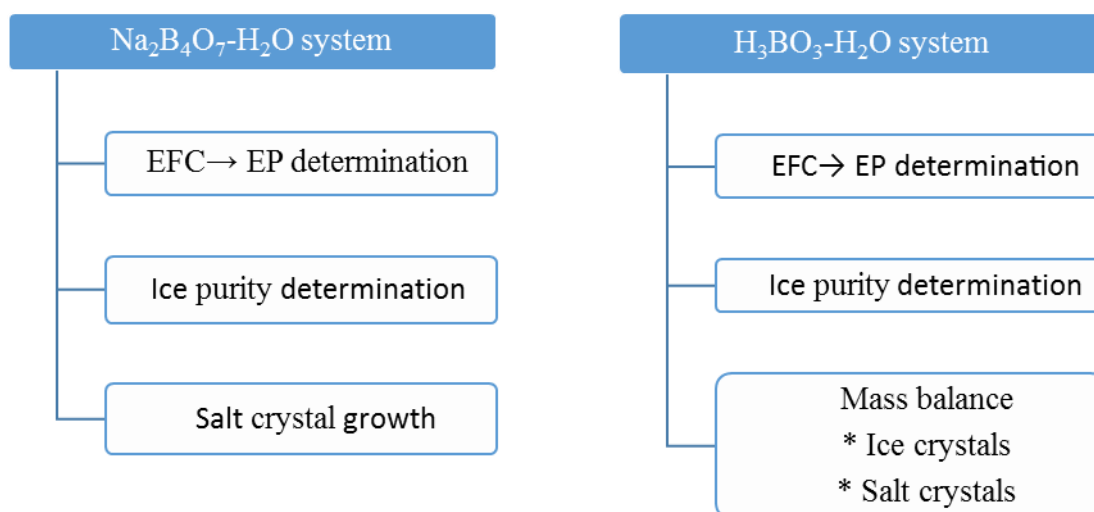


Figure 4.1 : Experimental investigations outline.

4.1 Investigations for Borax-water ($\text{Na}_2\text{B}_4\text{O}_7\text{-H}_2\text{O}$) System

EFC → EP determination: 2 wt% borax solution was employed for investigation of eutectic point. The temperature inside the crystallizer (T1) and the temperature between the crystallizer and the double walled vessel (T2) were recorded as a function of time as shown in Figure 4.2. Starting from room temperature, the borax solution temperature (blue line) decreased due to the decline in coolant temperature (orange line). As seen in the Figure 4.2, the salt nucleation was not obtained in the temperature profile, also not observed during the experiment. However, the ice nucleation moment was obtained in temperature profile. When ice nucleation occurred, the temperature increased due to the released heat of crystallization. Upon

cooling, it reached to the eutectic point, which was recorded as $-0.74\text{ }^{\circ}\text{C}$. Hence, eutectic point is the lowest temperature that the ice, salt and solution can thermodynamically exist all together, the crystallizer temperature is kept constant until all the system solidifies. This is also confirmed in Figure 4.2. As eutectic point is reached, the system temperature is kept constant. At the eutectic point the temperature difference between the coolant and solution temperature ($\Delta T = \approx 6\text{ }^{\circ}\text{C}$) is the driving force for the nucleation and growth of ice and salt crystals.

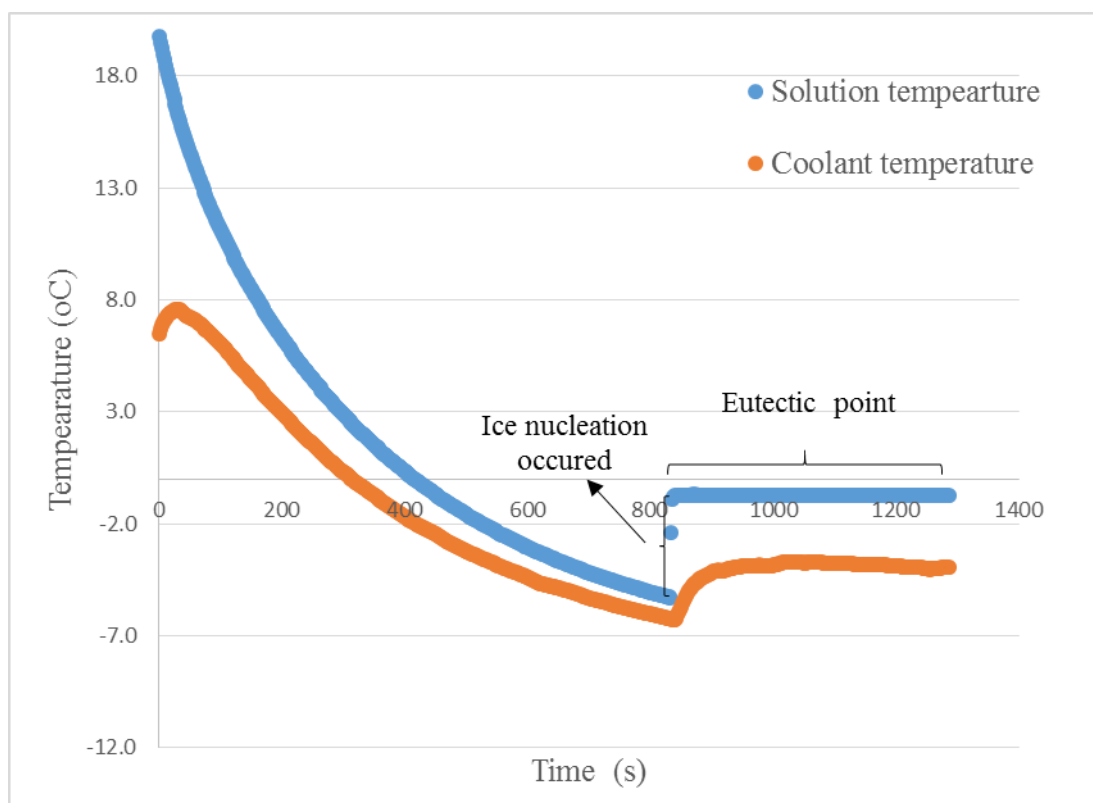


Figure 4.2 : Temperature-Time diagram of borax.

Borax-water solubility curve was plotted from Seidell's solubility data [45] and presented in Figure 4.3. Blue and orange lines represent the borax equilibrium, and ice equilibrium lines respectively. The gray spot on the figure represents the starting solution's composition (2 wt% borax) and temperature (at room temperature).

11 experiments were conducted in total following the procedure presented in Section 3.2.2. Determining the temperature via the temperature measurements and the concentration via the titration analysis, the eutectic point of $\text{Na}_2\text{B}_4\text{O}_7\text{-H}_2\text{O}$ system (which is the intersect of ice-borax equilibrium lines) was detected to be 1.06% $\text{Na}_2\text{B}_4\text{O}_7$ and $-0.74\text{ }^{\circ}\text{C}$.

According to Seidell data [45], the salt which is crystallized under eutectic conditions is in borax decahydrate ($\text{Na}_2\text{B}_4\text{O}_7 \cdot 10\text{H}_2\text{O}$) form. We could not confirm this information due to the lack of cryo-single crystal XRD analysis facility at our laboratory.

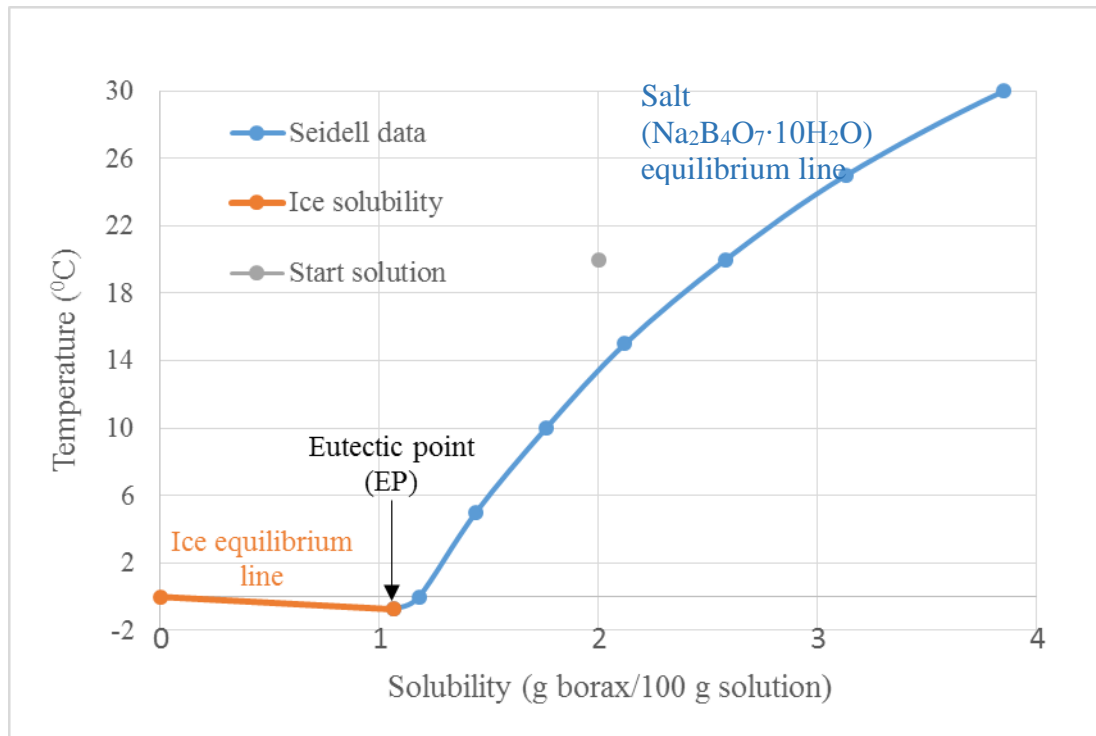


Figure 4.3 : Concentration-Temperature diagram for borax.

Ice purity determination: To understand the quality of ice product under eutectic conditions, we checked the purity of ice via vacuum filtration and washing experiments. We could also have checked the salt purities under EFC. However, since these experiments aimed to evaluate the applicability of EFC technology for the boron component systems, these first set of experiments were performed only by using pure borax and boric acid raw materials instead of industrial streams with high impurities. Thus the purity determination of salt crystals were not investigated both for borax and boric acid systems.

After reaching eutectic point, the system was operated under batch eutectic conditions for about 1 hour at a temperature difference (between the coolant and solution) of $\Delta T \approx 6$ °C. Ice and salt crystals nucleated and grew in the crystallizer during this time. After 1 hour, stirrer was stopped, and ice and $\text{Na}_2\text{B}_4\text{O}_7 \cdot 10\text{H}_2\text{O}$ salt crystals were separated due to their density differences as shown in Figure 4.4. This

is also confirmed by their densities from the literature; ice (0.92 g/cm^3), $\text{Na}_2\text{B}_4\text{O}_7 \cdot 10\text{H}_2\text{O}$ salt crystals (1.73 g/cm^3) [45], [47]. $\text{Na}_2\text{B}_4\text{O}_7$ solution (1.06 g/cm^3) density at eutectic point which was measured during the context of this thesis with Density Meter DMA 35. Its accuracy of density was 0.001 g/cm^3 . It can be seen that salt crystals settle at the bottom of the crystallizer and ice crystals float at the top. The crystallization process was followed by vacuum filtration of ice. Sample from the ice cake on the filter and filtrated solution were collected and weighted. Then the ice crystals were washed with pre-cooled till $0 \text{ }^\circ\text{C}$ 50 ml de-ionized water. After each washing step, samples of the ice on the filter and the filtered solutions were collected and weighted. 2 washing steps were performed in total both for borax-water and boric acid-water systems. All the collected samples were titrated for composition determination. Salt amount was confirmed after each washing step via the mass balance analysis.

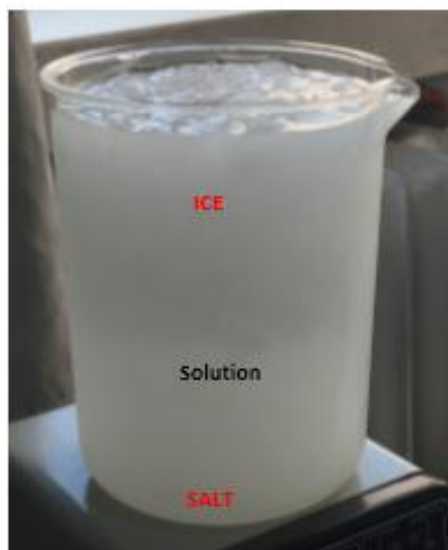


Figure 4.4 : $\text{Na}_2\text{B}_4\text{O}_7 \cdot 10\text{H}_2\text{O}$ salt-ice and $\text{Na}_2\text{B}_4\text{O}_7$ aqueous solution separation.

In Figure 4.5, the result of vacuum filtration and washing process is given as a graph. It can be seen that the amount of $\text{Na}_2\text{B}_4\text{O}_7$ in the un-washed solution from the crystallizer is at eutectic composition. Ice directly filtrated from the crystallizer (un-washed) had a significant amount of $\text{Na}_2\text{B}_4\text{O}_7$ composition. This can either originate from the mother liquor surrounding the ice crystals or the salt crystals captured in (due to crystal defect) or within the ice crystals (due to inefficient settling in the crystallizer). To improve the ice product quality and understand the origin of

$\text{Na}_2\text{B}_4\text{O}_7$ composition, as we said washing steps were conducted. It can be seen in Figure 4.5 that, after each washing step the $\text{Na}_2\text{B}_4\text{O}_7$ composition of ice and filtrate decreased. After 2nd washing step, the ice crystals (i.e. water) reached to 0.06% impurity. This decreasing trend in $\text{Na}_2\text{B}_4\text{O}_7$ composition shows that, salt crystals were not captured within the ice crystals but rather surrounding mother liquor was the reason.

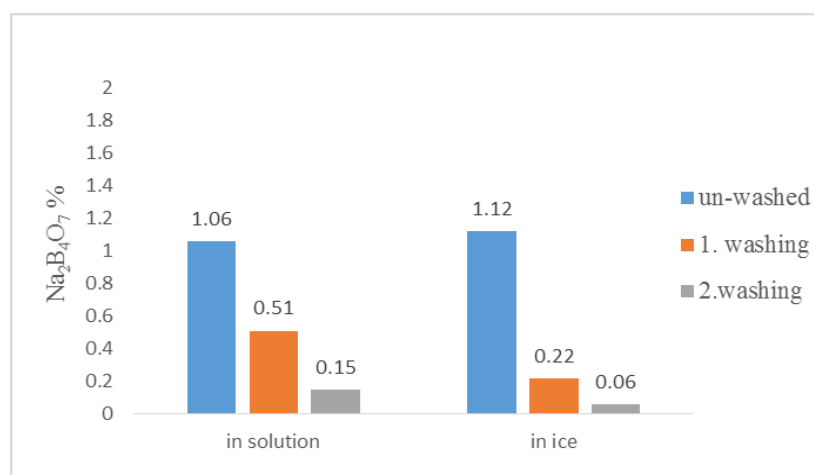


Figure 4.5 : $\text{Na}_2\text{B}_4\text{O}_7$ % amounts in solution and ice, after filtration and washing steps.

Crystals: As seen in Figure 4.6 the shape and size of $\text{Na}_2\text{B}_4\text{O}_7 \cdot 10\text{H}_2\text{O}$ salt crystals were rectangular (or elongated prisms) and small approximately 20 μm . The shape of salt crystals matches well with the literature data [35]. Ice crystal seemed to be roughly circular shaped with a size range around 80-100 μm . During the experiments, it was observed that the salt crystal was incorporated in ice.

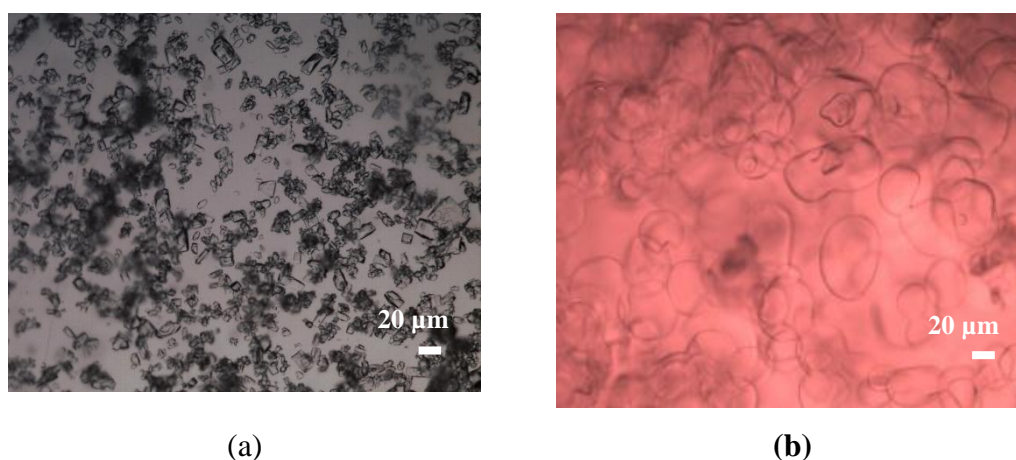


Figure 4.6 : (a) $\text{Na}_2\text{B}_4\text{O}_7 \cdot 10\text{H}_2\text{O}$ salt (b) ice crystal image.

During the experiments due to small sizes of the salt crystals, the inefficient separation from ice was observed. This was the biggest obstacle in all performed experiments. The salt crystals captured in the ice as seen in Figure 4.7, caused several more difficulties such as salt remain in the suspension without settling. This creates a difficulty for solution collection from the crystallizer for concentration determination, as well.

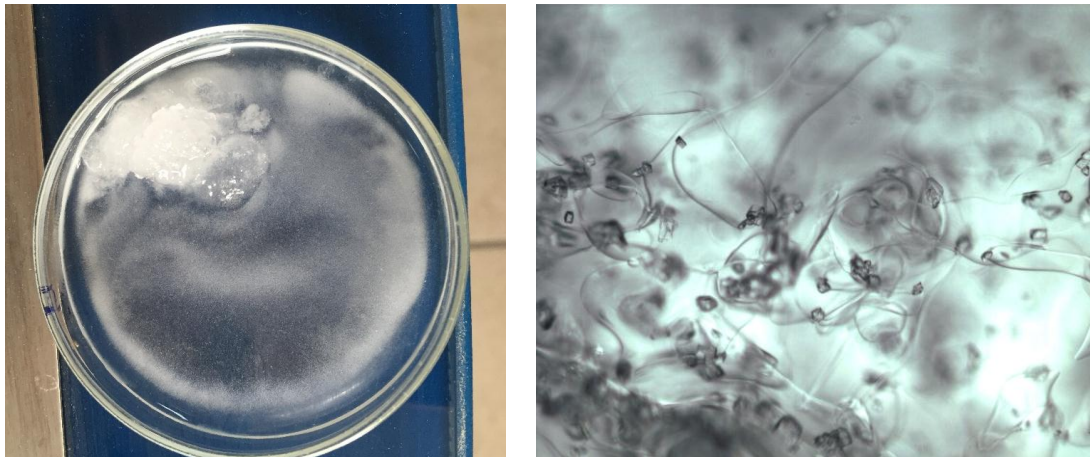


Figure 4.7 : The salt ($\text{Na}_2\text{B}_4\text{O}_7 \cdot 10\text{H}_2\text{O}$) captured in the ice photos.

Therefore, kinetic information from the $\text{Na}_2\text{B}_4\text{O}_7 \cdot 10\text{H}_2\text{O}$ salt growth rate was investigated further under different batch eutectic conditions for different supersaturations.

Salt crystal growth: For unseeded-crystal size measurement experiments microscopic photos taken at different range of time and at different coolant set temperatures are shown in Table 4.1.

After measuring each crystal area taken under microscope, using Image J program, a characteristic radius for each ΔT (supersaturation) was calculated. For different batch times, characteristic radiuses were defined and their relations are presented in Figures 4.8-4.9-4.10.

For doing these, the following assumptions were made.

- The supersaturation (ΔT) is defined as follows:
$$\Delta T = (T_{\text{eutectic inside the crystallizer}}) - (T_{\text{coolant in between crystallizer and double walled vessel}})$$
- Crystal agglomeration and breakage are absent,
- Crystals are born in the lowest particle class as secondary nucleation,

- Growth rate is size-independent,
- Homogenous stirring in the crystallizer,
- System is not operated continuous but batch. Thus system is operating under unsteady state conditions; number of crystals are increasing over time. In our calculations, the error one can make in the growth rate calculations due to batch operation is neglected.

Table 4.1 : Crystal size measurement and calculation results.

T_{CM} (°C)	ΔT (°C)	Batch time (s)	# counted crystals	A_{avg} (μm)	r (μm)	GR ($\mu m/s$)
-7	4.94	600	350	542	16.05	0.003
-7		1800	400	1390	10.08	
-7		3600	340	579	19.48	
-7		18000	200	397	63.13	
-8.5	5.26	600	350	46.2	7.36	0.0032
-8.5		1800	400	466	12.14	
-8.5		3600	300	147	23.47	
-8.5		18000	300	407	64.86	
-10	6.46	600	300	52.9	8.43	0.0033
-10		1800	300	61.6	9.81	
-10		3600	300	131	20.81	
-10		18000	300	410	65.24	

T_{CM} = Cooling machine set temperature

ΔT = $T_{coolant}$ in between crystallizer and double walled vessel - T_{eut}

A_{avg} : Average area

r: Characteristic radius

Using Figure 4.8-4.10, by linearizing the characteristic radius value versus time, a growth rate ($\mu m/s$) was defined for each supersaturation. Growth rate was defined as the slope of the linearized experimental data. These values are shown both on the related Figures and in Table 4.1. The defined growth rates of borax decahydrate crystals were then presented as a function of supersaturations in Figure 4.11. In our defined supersaturation ($\Delta T \approx 5-6$ °C) range, the growth rate of $Na_2B_4O_7 \cdot 10H_2O$ crystals were found to be around 3×10^{-9} m/s. Compared to other hydrated inorganic salts, this value is a bit slow [35]. As seen in Figure 4.11, the relation between the supersaturation and growth rate is detected to be linear. This investigation is in parallel with the results of Suharso, where he detected a linear growth rate relation of borax crystals from bulk experiments above a critical relative supersaturation ($1/(S-1)$) of 0.3 [49]. It has to be noted that in Suharso's work, the definition of

supersaturation is different from our work. He indicated that above the relative supersaturation of 0.3, birth and spread mechanism is dominating the crystal growth. For all supersaturations, after 5 hours of batch operation, $\text{Na}_2\text{B}_4\text{O}_7 \cdot 10\text{H}_2\text{O}$ crystal size distribution was around $65 \mu\text{m}$. This identical average salt size might be due to the close supersaturation (ΔT) values in 3 different experiments. The larger the crystals, the easier they settle in the crystallizer under EFC conditions. Thus, this larger crystal size distribution might improve its separation behaviour from ice.

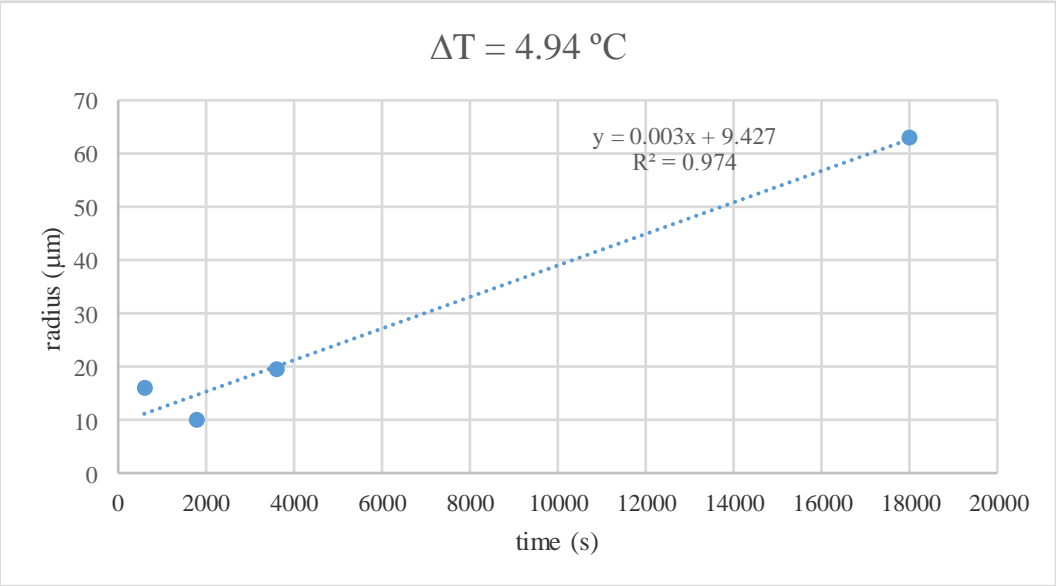


Figure 4.8 : Time versus Characteristic Radius Graph for $\Delta T=4.94 \text{ }^\circ\text{C}$.

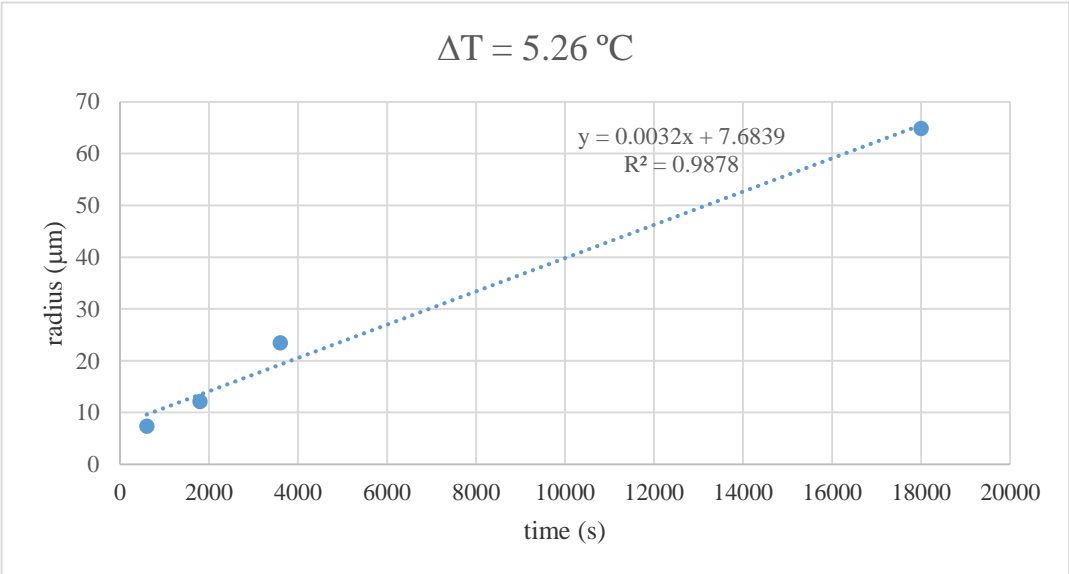


Figure 4.9 : Time versus Characteristic Radius Graph for $\Delta T=5.26 \text{ }^\circ\text{C}$.

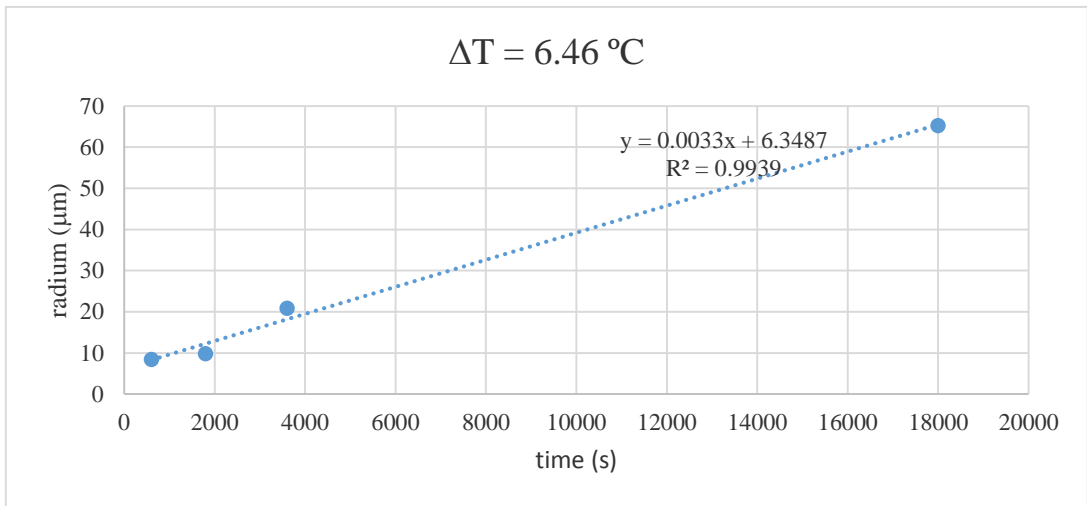


Figure 4.10 : Time versus Characteristic Radius Graph for $\Delta T=6.46$ °C.

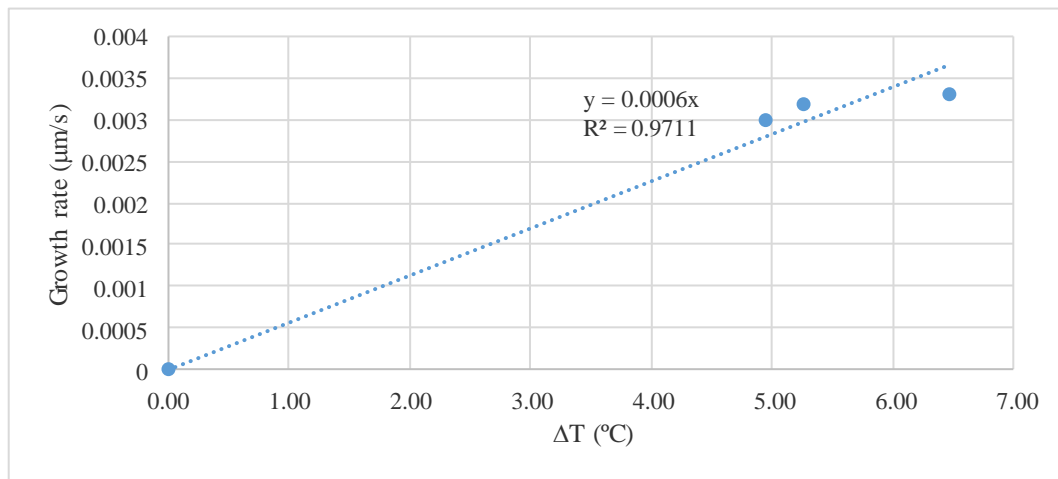


Figure 4.11 : Supersaturation (ΔT)-Growth Rate Graph for $\text{Na}_2\text{B}_4\text{O}_7 \cdot 10\text{H}_2\text{O}$ crystals.

4.2 Investigations for Boric Acid-Water ($\text{H}_3\text{BO}_3\text{-H}_2\text{O}$) System

EFC → EP determination: An aqueous solution of 2.5 wt% boric acid was employed for investigation of eutectic point. For boric acid-water system, same experimental design and procedure was used with the borax-water system. In the temperature profile presented in Figure 4.12, the temperature jump represents the ice nucleation moment. Similar to borax case, during all the performed experiments salt nucleation point was not observed in the temperature profile as a jump. This might be due to little amount of salt crystallization. So the heat of crystallization of the nucleated salts were not enough to effect the solution's temperature. Salt crystals nucleated before ice crystals occurred. As soon as ice crystals nucleated, the system reached to eutectic point. Eutectic temperature of boric acid-water solution was

detected to be $-0.75\text{ }^{\circ}\text{C}$. This eutectic temperature is close to literature value ($-0.76\text{ }^{\circ}\text{C}$) measured by Nasini and Ageno [45]. In general after reaching eutectic point, the crystallizer temperature keeps constant. This fact was also confirmed for boric acid-water system as seen in Figure 4.12.

Both initial and eutectic concentrations of boric acid were measured with titration. In a typical experiment the eutectic concentration of the sample was detected to be 2.5 wt% (25.14 g/L). This value is in good agreement with the literature value which is 2.46 wt. % (24.6 g/L) [45].

According to Seidell data [45], the salt which is crystallized under eutectic conditions is in boric acid (H_3BO_3) form.

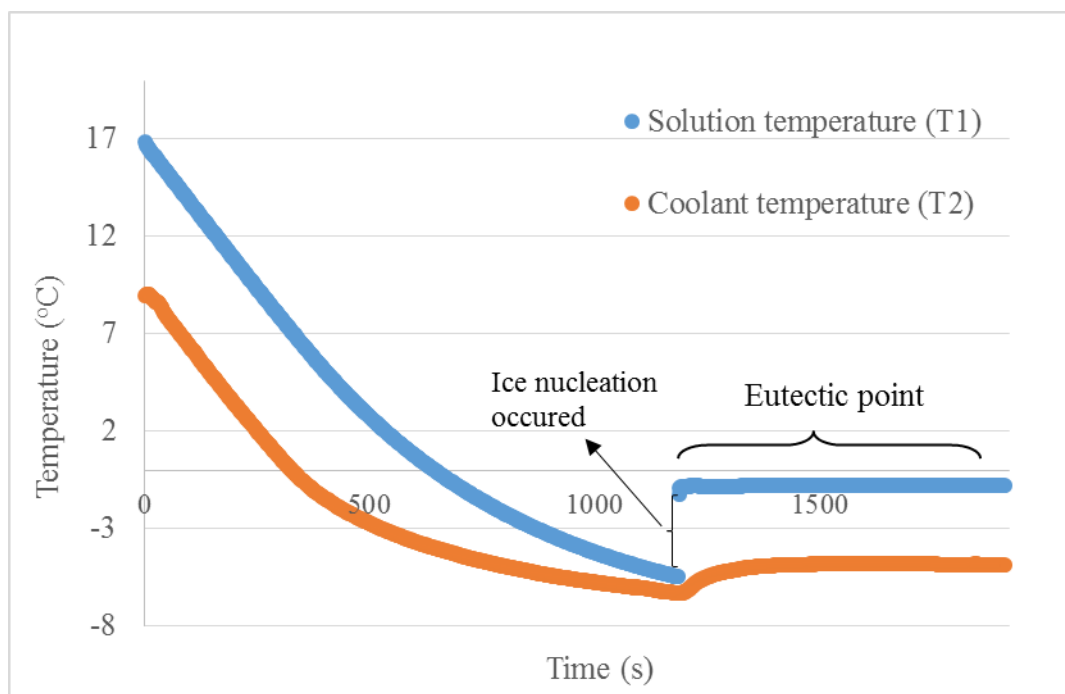


Figure 4.12 : Temperature-Time diagram of boric acid.

Boric acid-water solubility curve was plotted from Seidell's solubility data [36] and presented in Figure 4.13. Blue line represents the boric acid equilibrium line, and orange line demonstrates the ice equilibrium line. We drew ice equilibrium line using pure water freezing point ($T_{\text{eq}@0^{\circ}\text{C}}$) and one experimental data for 0.5% H_3BO_3 ($T_{\text{eq}@-0.28\text{ }^{\circ}\text{C}}$). The gray spot on the figure represents the starting solution (2.5 wt% boric acid) at room temperature.

Based on our first experiments detected eutectic point (yellow point) is shown in the figure. As seen, our detected point seems to be more accurate compared to the literature value and fulfills the diagram better.

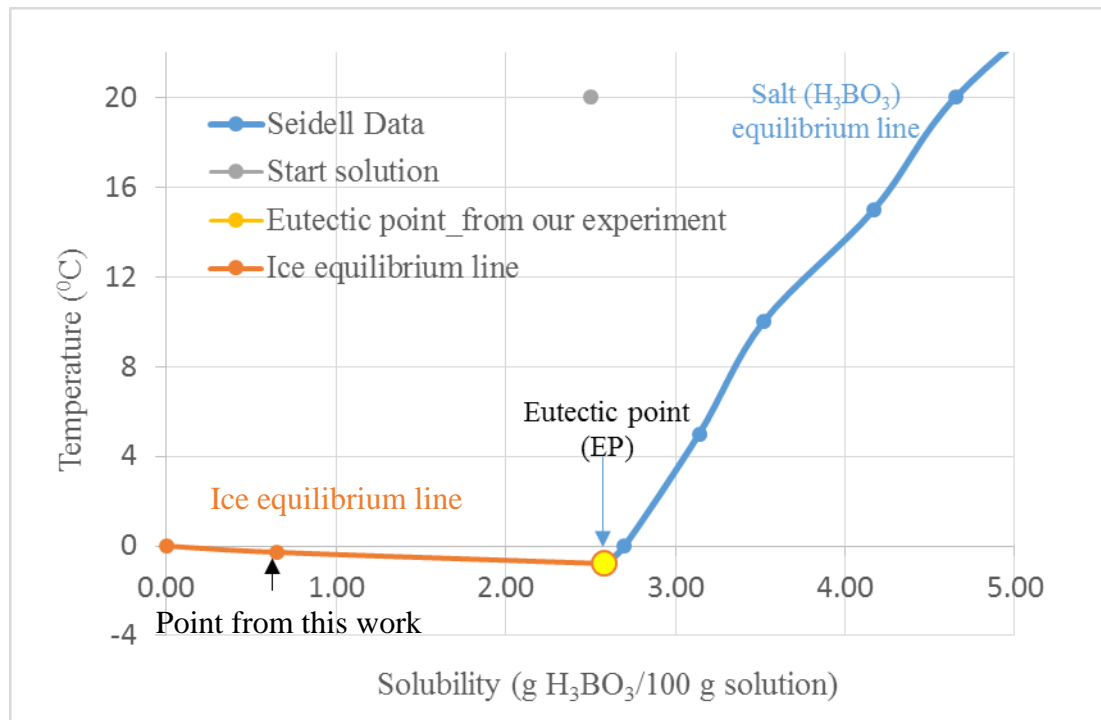


Figure 4.13 : Concentration-Temperature diagram for boric acid.

Ice purity determination: Similar to borax case the quality of ice product under eutectic conditions was investigated using vacuum filtration and washing experiments. For the same reason discussed above, the salt purities were not studied.

After reaching to the eutectic point, between the crystallizer and ethylene glycol solution temperature was kept constant almost at/around 4 °C. This temperature difference was a driving force (ΔT) for ice and salt crystals nucleation and growth.

Under eutectic conditions, ice and salt crystals grew for 20 minutes due to the driving force ($\Delta T = 4$ °C). Then the stirrer was stopped; consequently, ice and boric acid salt crystals were separated from each other by their density difference (Figure 4.14) similar to borax case. Ice crystals float, salt crystals settle. According to literature, ice, salt and the solution densities are 0.92 g/cm³, 1.44 g/cm³, and 1.005 g/cm³ respectively [47], [32]. After separation, boric acid was detected in the ice and solution by washing and filtering procedures.



Figure 4.14 : Boric acid salt-ice and solution at the eutectic point.

For a typical experiment, ice (un-washed and 2 times washed) and solution (un-washed-filtered ice solution, and washing solution after each washing step) results are presented in Figure 4.15. The mother liquor contained 2.58 wt% boric acid; which is the eutectic composition. The filtered ice had a boric acid composition of 2.22 wt%. This value shows that the ice crystals either contain or surrounded by the mother liquor, and/or salt crystals were captured in between the ice crystals. As for the borax case, the origin of this composition can only be understood by the washing procedure. Thus the filtered ice was washed twice using 0 °C pre-cooled pure water. As seen in Figure 4.15, boric acid concentration of the ice crystals decreased after each washing step. This shows that same as for borax case, mother liquor was not captured within the ice crystals, but it covered the surface of the ice. Besides, the salt crystals possibly were not settled effectively but instead floated together with the ice due to their small size distribution as will be presented in the following lines.

After 2 times washing, the boric acid composition of the ice crystals was decreased to 0.83 wt% which is good enough to be used as a process water. As seen in Figure 4.15, solution in filtering process also has a decreasing profile. This is another indication proving the impurities not building within the ice but instead surrounding the ice crystals. If they were to be captured, then the expected profile would be constant after each washing step.

Compared to borax case, our washing steps were less efficient. The purity of ice crystals can further be enhanced by improving the washing procedure, increasing the washing steps or performing the washing steps in a cold room.

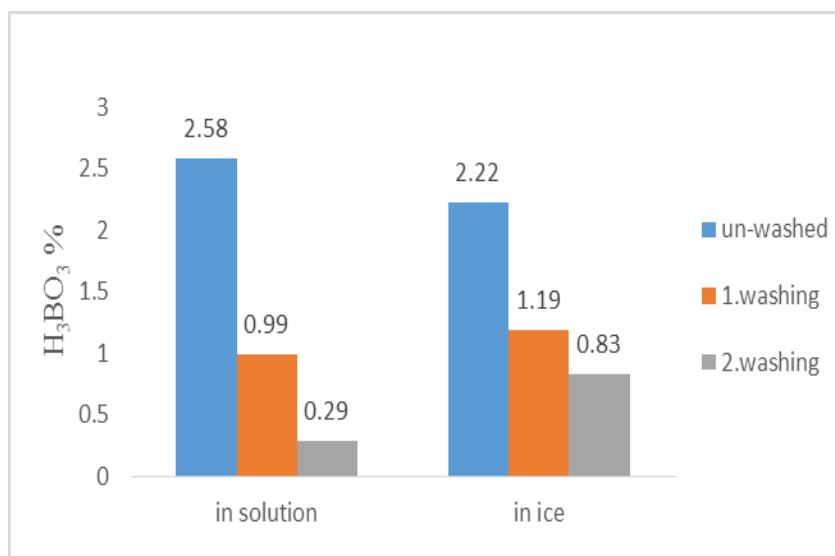


Figure 4.15 : H_3BO_3 % amounts in solution and ice, after filtration and washing steps.

Crystals: Samples of the crystals were observed under the microscope using the 5X camera. In Figure 4.16 the results can be seen. Boric acid salt crystals were square like with an average size range around 5-10 μm . According to literature, they are mostly in needle shape [35]. In our experiments since they were very small, they probably did not have a proper habit. According to the Figure 4.16, they were smaller crystals. In terms of the ice crystals, the shape was round and the size was around 15-30 μm .

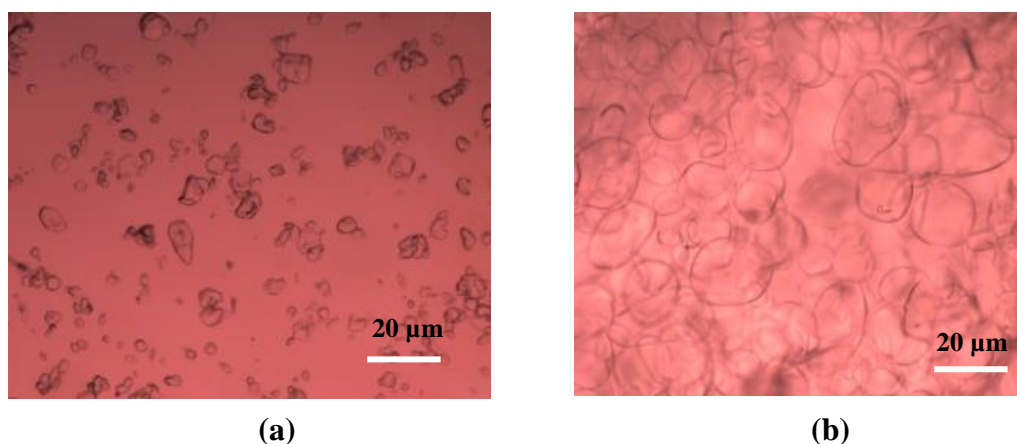


Figure 4.16 : (a) H_3BO_3 salt (b) ice crystal image.

Mass balance: Boric acid-water system was operated under eutectic conditions at/around 4 °C supersaturation for 20 min. Since there was no efficient separation of ice and salt within the crystallizer, the boric acid salt and ice production amounts could not be detected exactly at the end of the experiment. Thus the boric acid amount in the final filtrated solution (13.7 g) was calculated and this amount was subtracted from the initial boric acid amount (20 g) which was used for preparing the starting solution. 6.3 grams of boric acid salt was calculated to be crystallized under eutectic conditions. In doing that, we assumed all the boric acid ended up in the bulk-ice, scaled-layer and the solution was in the crystalline form. Details of this calculation is given in Appendix B. (The locations of bulk-ice, scaled-layer and the solution can be found in Appendix Figure B.1).

4. CONCLUSIONS

In this work, new EFC technology was successfully tested on 2 wt% borax and 2.5 wt% boric acid aqueous solutions. The experiments were investigated in a 1 liter batch crystallizer.

First set of experiments were conducted for determination of eutectic points for borax-water system ($\text{Na}_2\text{B}_4\text{O}_7\text{-H}_2\text{O}$). The eutectic point was found as 1.06 wt% $\text{Na}_2\text{B}_4\text{O}_7$ and -0.74 °C. In literature, eutectic point of borax-water system is not documented before.

Eutectic composition of boric acid-water ($\text{H}_3\text{BO}_3\text{-H}_2\text{O}$) system was also investigated. Its eutectic point was detected to be 2.51 wt% (25.14 g/l) H_3BO_3 at -0.75 °C. This value is close to the Siedell data with -0.76 °C and 2.46 wt% (24.6 g/l).

After reaching eutectic point, borax and boric acid systems were treated under eutectic conditions for 60 and 20 minutes, respectively.

Borax decahydrate salt crystals ($\text{Na}_2\text{B}_4\text{O}_7\cdot 10\text{H}_2\text{O}$), investigated under microscope, had rectangular shapes with an average crystal size of 20 μm . The ice crystals were round and had around 80-100 μm size. Within the crystallizer not an efficient separation was observed due to the small size distribution of the salt crystals. Thus, salt crystals mostly ended up in the ice.

Boric acid crystals (H_3BO_3), having square like shape, had 5-10 μm average crystal sizes. This value was smaller compared to borax crystals due to the shorter batch time we applied. Ice, crystallized under eutectic boric acid crystallization, was in round shape and had around 15-30 μm size. Similar to borax case, the salt crystals were not settled in the crystallizer but rather held in the ice crystals due to their small sizes.

The floated and recovered ice (water), produced via eutectic freeze crystallization, has quite significance due to its economical and environmental impacts. Thus its quality was further investigated, both for borax and boric acid systems, within the scope of this thesis. The crystallized ice under EFC conditions were filtrated via vacuum filtration and washed with pre-cooled distilled water in two steps. After second washing, ice purities were reached to 0.06% and 0.83% for borax and boric acid systems, respectively. These ice (water) qualities are good enough to be used for process water. During washing steps, the hold up of salt crystals within the ice was also confirmed for both systems.

Under EFC operation, or improving the separation efficiency of boron salts from ice crystals, investigations were employed for the crystal growth of borax decahydrate salts. Under eutectic batch operation conditions, for about 5 °C of supersaturation (defined to be temperature difference between the coolant and the crystallizer), the crystal growth of $\text{Na}_2\text{B}_4\text{O}_7 \cdot 10\text{H}_2\text{O}$ were detected to be $\approx 3 \times 10^{-9}$ m/s. This value is relatively small compared to most of the other inorganic salts. Experimental results gave a linear relation between the supersaturation and the growth rate which is in parallel with literature. As proposed by Suharso, probably birth and spread mechanism is dominating the borax crystal growth. For confirmation of this information, further investigation can be done. After 5 hours of batch operation, salt crystals reached around 65 μm sizes, which is an improvement for its separation behaviour from the ice crystals.

These first sets of batch EFC experiments for borax and boric acid systems show that, instead of dumping to the ponds, treating via eutectic freeze crystallization, valuable products such as water and borax decahydrate/boric acid salts can be recovered from the industrial waste streams.

The quality of produced ice can further be developed by improving the filtration procedure. During this study salt crystals' quality and purity was not investigated elaborately. This can further be investigated in a following study.

6. RECOMMENDATIONS

These first set of experiments prove the basic principle of eutectic freeze crystallization technology for borax and boric acid waste streams and show its potential for treating boron containing streams.

In further studies, borax and boric acid crystal size distribution enlargements can be investigated more elaborately for improving the separation performance and salt product qualities of eutectic freeze crystallization. Results can be improved by performing the experiment, separation, filtration and washing steps in a cold room. This will prevent the disadvantageous that might be caused due to environmental effects.

REFERENCES

- [1] **Jansen, L.H.**, 1999, boron Compounds, Kirk-Othmer Encyclopedia of Chemical Technology, Vol 4, John Wiley & Sons, pp 337.
- [2] **Yakar, E.I.** 2004, Utilization of Industrial Borax Wastes (BW) for Portland cement production, TÜBİTAK Turkish J. Eng. End. Sci. 28 (2004), 281-287.
- [3] **Kavas, T et al.**, 2011, Valorisation of different types of boron-containing wastes for the production lightweight aggregates, Journal of Hazardous Materials 185 (2011) 1381-1389.
- [4] **Uslu, T., Arol, A.I.**, 2004, Use of boron waste as an additive in red bricks, Waste Management 24 (2004) 217-220.
- [5] **Kurama, S., Kara, A., Kurama, H.**, 2006, The effect of boron waste in phase and microstructural development of a terracotta body during firing, Journal of the European Ceramic Society 26 (2006) 755-760.
- [6] **Gorenflo, A., Velázquez-Padrón, D., Frimmel, F.H.**, 2003, Nanofiltration of a German groundwater of high hardness and NOM content: performance and cost, Desalination, 151 (2003) 253-265.
- [7] **Walha, K., Amar, R.B., Firdaous, L., Quéméneur, F., Jaouen, P.**, 2007, Brackish groundwater treatment by nanofiltration, reverse osmosis and electro dialysis in Tunisia: performance and cost comparison, Desalination, 207 (2007) 95-106.
- [8] **Snyder, S.A., Adham, S., Redding, A.M., Cannon, F.S., DeCarolis, J., Oppenheimer, E.C., Wert, E.C., Yoon, Y.**, 2007, Role of membranes and activated carbon in the removal endocrine disruptors and pharmaceuticals, Desalination, 202 (2007) 156-181.
- [9] **Radjenović, J., Petrović, M., Ventura, F., Barceló, D.**, 2008, Rejection of pharmaceuticals in nanofiltration and reverse osmosis membrane drinking water treatment, Water Research, 42 (2008) 3601-3610.
- [10] **Salvador Cob, S., Genceli, F.E., Hofs, B., Witkamp, G.J.**, 2014, Three strategies to treat reverse osmosis brine and cation exchange spent regenerant to increase system recovery, Desalination, 344:36-47.
- [11] **Angulo, A.M.**, 2001, Boron. U.S Geological Survey, 2009 Minerals Yearbook, USGS.
- [12] **Gale, W.A.**, 1961, Development and present status of the borax industry. American Potash and Chemical Corp., Whittier, California.
- [13] **Wolska, J., Bryjak, M.**, 2013, Methods for boron removal from aqueous solutions: A review, Desalination, 310 18-24.
- [14] **Eti Maden İşletmeleri Genel Müdürlüğü**, 2008, Boron, Faaliyet Raporu. Ankara.

- [15] **Kistler, R.B., Helvaci, C.**, 1994, Boron and borates. In industrial Minerals and Rocks, 6th ed. pp 171-186.
- [16] **Info Mine research group**, 2009, Boron and Borates Market Research in the CIS. Moscow.
- [17] **Stormcrow**, 2015, Industry report/ Borates, Retrieved; May 2, 2016 from www.stormcrow.ca/research.
- [18] **Eti Maden İşletmeleri Genel Müdürlüğü**, 2014, Bor Sektor Raporu 2013, Ankara.
- [19] **Helvaci, C., Alonso, N.R.**, 2000, Borate Deposits of Turkey and Argentina: A Summary and Geological Comparison. Turkish Journal of Earth Science. Vol. 9. pp. 1-27.
- [20] **Bayca, S.U.**, Recovery of boric acid from colemanite waste by sulfuric acid leaching and crystallization. University of Celal Bayar, Soma Vocational School, Soma, 45500 Manisa, Turkey.
- [21] **Risk and Policy Analysts**, 2008, Assessment of the Risk to Consumers from Borates and the Impact of Potential Restrictions on their Marketing and Use, UK.
- [22] **Rio Tinto Mineral Outlook**, 2015, Rio Tinto: Global outlook for borates, Industrial minerals. USA.
- [23] **Gülçek, A.H., Meriç, A.**, Boraks pentahidrat prosesinde yapılan iyileştirme çalışmaları, Eskişehir.
- [24] **Yorulmaz, A.**, 2004, Tinkal cevherinden Nitrik Asit Kullanarak Boric Asit Üretim Prosesinin Geliştirilmesi, Yüksek Lisans Tezi, İTÜ Fen Bilimleri Enstitüsü, İstanbul.
- [25] **Bentli, T., Ediz, N., Özdemir, O.**, Bor Atıkları ve Değerlendirilme Stratejileri, Turkey.
- [26] **Özdemir, M., Öztürk, N.U.**, 2003, Utilization of clay wastes containing boron as cement additives, CRR Journal, 33, pp 1659-1661.
- [27] **Mineral processing technology (MPT-2005)**, 2005, Department of Fuel and Mineral Engineering, Indian School of Mine, Dhanbad.
- [28] **Kırka plant project**, Eti Mine. Retrieved; May 2, 2016 from <http://www.csb.gov.tr>.
- [29] **United Nations**, 2007, United Nations Environment Programme/Grid-Arendal. Maps and Graphics, Retrieved; May 2, 2016 from <http://www.maps.grida.no>.
- [30] **Genceli, F.E.**, 2008, Scaling-Up Eutectic Freeze Crystallization, PhD dissertation, Delft University of Technology, Netherland.
- [31] **Schubert, M.D.**, 2015, Boric Oxide, Boric acid, and Borates, Ullmann's Encyclopedia of industrial chemistry, Rio Tinto Greenwood Village, Colorado, USA.
- [32] **Walter, C.B.**, 1939, The solubility curves of boric acid and the borates of sodium, Chemical laboratory of the University California, USA.

- [33] **Tavare, N.**, 1995, Industrial crystallization: Process Simulation Analysis and Design, Plenum Press, New York.
- [34] **Aamir, E.**, 2010, Population Balance model-based optimal control of batch crystallization processes for systematic crystal size distribution design, PhD dissertation, Loughborough University, UK.
- [35] **Mullin, J.W.**, 2001, Crystallisation, Butterworth Heinemann, London, UK.
- [36] **Wojciech, B., Januez, W.**, 2014, The metastable zone of aqueous solutions, X Conference Chances and possibilities of chemical industry in EU, Silesian University of Technology, Poland.
- [37] **Ulrich, J., Jones, M.J.**, Heat and mass transfer operations- crystallization, Chemical engineering and chemical process technology (EOLESS), Martin-Luther University, Germany.
- [38] **Myerson, A.S.**, 1993, Handbook of Industrial Crystallization, Butterworth-Heinemann, London.
- [39] **Lu, X.**, 2014, Novel Applications of Eutectic Freeze Crystallization, PhD dissertation, Delft University of Technology, Netherland.
- [40] **Pascual, M.R.**, 2009, Physical Aspects of Scraped Heat Exchange Crystallizer: an Application in Eutectic Freeze Crystallization, PhD dissertation, Delft University of Technology, Netherland.
- [41] **Vaessen, R., Seckler, M., Witkamp, G.J.**, 2003, Eutectic Freeze Crystallization with an aqueous $\text{KNO}_3\text{-HNO}_3$ solution in a 100 L cooled-disk column crystallizer. *Ind Eng Chem Res*, 42(20): 4874-4880.
- [42] **Genceli, F.E., Gärtner, R., Witkamp, G.J.**, 2005a, Eutectic Freeze Crystallization in a 2nd Generation Cooled Disk Column Crystallizer for $\text{MgSO}_4\cdot\text{H}_2\text{O}$ System, *Journal of Crystal Growth*. 2005, 275(1-2), e1369-e1372.
- [43] **John, A.S., Earl, C.H.**, 1943, Freezing points, Densities, and Refractive indexes of the System Glycerol-Ethylene Glycol-Water, West Virginia University, Morgantown.
- [44] **Genceli, F.E., Wahlin, J., Hinge, M., Kjelstrup, S.**, 2015, The temperature jump at a growing ice –water interface, *Chemical Physics letters*, Vol 622, 16 Feb 2015, pp 15-19.
- [45] **Seidell, A., Linke, W. F.**, 1965, Solubilities of Inorganic and Metal Organic Compounds, Fourth Edition, American Chemical Society, Washington, D.C.
- [46] **Image Pro Plus user manual**. Retrieved; May 2, 2016 from <http://www.mediacy.com/imageproplus>.
- [47] **Dallas, A.**, 2000, <http://hypertextbook.com/facts/2000/AlexDallas.shtml>.
- [48] **Franson, M.A.H.** 1992, Standart Methods for the Examination of Water and wastewater, 2/36 – 2/38, Eds. Greenbers, A.E., Clesceri, L.S., Eaton, A.D., American Public Health Association Water Environment Federation.

- [49] **Suharso.**, 2008, Mechanism of borax crystallization using conductivity method, *Indo.J, Chem.*, 2008, 8 (3), 327-380.

APPENDICES

Appendix A: Eutectic Freeze Crystallization Determination experiments' measurements.

Appendix A.1: Water-Ethylene Glycol concentration and freezing point relations was used in experiment.

Appendix A.2 : Determination of Borax and Boric Acid Concentration by Titration.

Appendix A.3 : Standardization of NaOH Solution.

Appendix A.4 : Concentration differences between actual and experiment measurements.

Appendix B : Details of a Mass and Component Balance of Filtration for boric acid.

Appendix C: Crystal Size Determination experiments' microscopic images for borax decahydrate.

Appendix D: Crystal Size Determination experiments' temperature profiles for borax decahydrate.

Appendix A : Eutectic Freeze Crystallization Determination experiments' measurements.

Appendix A.1 : Water-Ethylene Glycol concentration and freezing point relations was used in experiment.

Table A.1 : Water-Ethylene Glycol concentration and freezing point relations.

Volumetric Mixture ratio	Freezing Point
100% Water	0 °C
90% Water+10% Glycol	-2.5 °C
80% Water+20% Glycol	-7.7 °C
70% Water+30% Glycol	13.9 °C
60% Water+40% Glycol	23.3 °C
50% Water+50% Glycol	33.9 °C

Appendix A.2 : Determination of Boric Acid Concentration in Solution by Titration.

Borax or Boric acid contents of each collected ice and solution sample were done by titration. 10 mL of samples were taken before the crystallization and after reaching the eutectic point for determining the concentration of borax or boric acid. First of all, methyl red indicator was dropped into the solutions. 1:1 HCl was added until the colour was changed to pink. This stage caused a decrease in the solution's pH. Solution contained CO₂; consequently, it had to be removed since boric acid is a weak acid and it might affect the result of titration. Therefore, solution was boiled and then cooled. Until the colour change, 1 N NaOH was added and a yellow colour was observed by addition of 0.1 N NaOH. After this step, three spoons of mannitol and four drops of phenolphthalein indicator were added. Afterwards titration was done with 0.1 N NaOH. Titration was continued until the pink colour was seen. At the end of the titration, the amount of used NaOH was determined. Borax or Boric acid concentration of the sample was determined using the following formula.

$$C = \frac{N \times M_A \times V_2}{V_1} \quad (\text{App.1})$$

Where

- C = Borax or Boric Acid Concentration (g/L)
- N = Normality of NaOH (N)
- M_A = Molecular weight of Borax or Boric Acid (g/mol)
- V₁ = Volume of sample (mL)
- V₂ = Used of NaOH (mL)

Appendix A-3 : Standardization of NaOH Solution.

To prepare 0.1 M NaOH, four grams of NaOH was weighed and completed to 1 L with addition of distilled water and mixed to dissolve. Potassium hydrogen phthalate ($C_8H_5KO_4$) was used for standardization to find the normality of 0.1 M NaOH. Approximately 1 gram of potassium hydrogen phthalate was dissolved in 100 mL of distilled water. Besides, 3 drops of phenolphthalein indicator were added to this solution. After this, titration was done with 0.1 N NaOH until colour change. Used NaOH amount was noted. With this standardization, NaOH normality was determined to be used for the calculation of boric acid concentration of the sample. Normality of NaOH solution was determined using the following formula.

$$A = \frac{B}{0.20423 \times C} \quad (\text{App.2})$$

Where A = Normality of NaOH solution (N)
 B = Amount of $C_8H_5KO_4$ (g)
 C = Consumed amount of NaOH (mL)

Appendix A-4 : Concentration differences between actual and experiment measurements.

$$\text{Error (\%)} = \frac{\text{Actual measurement} - \text{Experimental measurement}}{\text{Actual measurement}} \times 100 \quad (\text{App.3})$$

Actual measurement: Prepared boric acid solution by weighting boric acid and water on a scale (error of scale ± 0.4 gram by Precisa XB 3200C).

The mean error is calculated as -4.7%. As presented in Table Appendix.A-2., errors change between the range of -8.99 and 1.77. Experimental measurements were greater than actual measurements; consequently, negative errors were obtained.

Table A.2 : Concentration differences.

Initial concentrations -actual measurement- (wt%)	Titration measurements -experimental measurement- (wt%)	Difference* (%)
2.49	2.49	0.44
2.50	2.59	-3.76
2.50	2.73	-8.99
2.50	2.46	1.77
2.50	2.69	-7.26
2.50	2.68	-7.14
2.50	2.66	-6.12
2.50	2.62	-4.71

*Scale error is not taken in to account

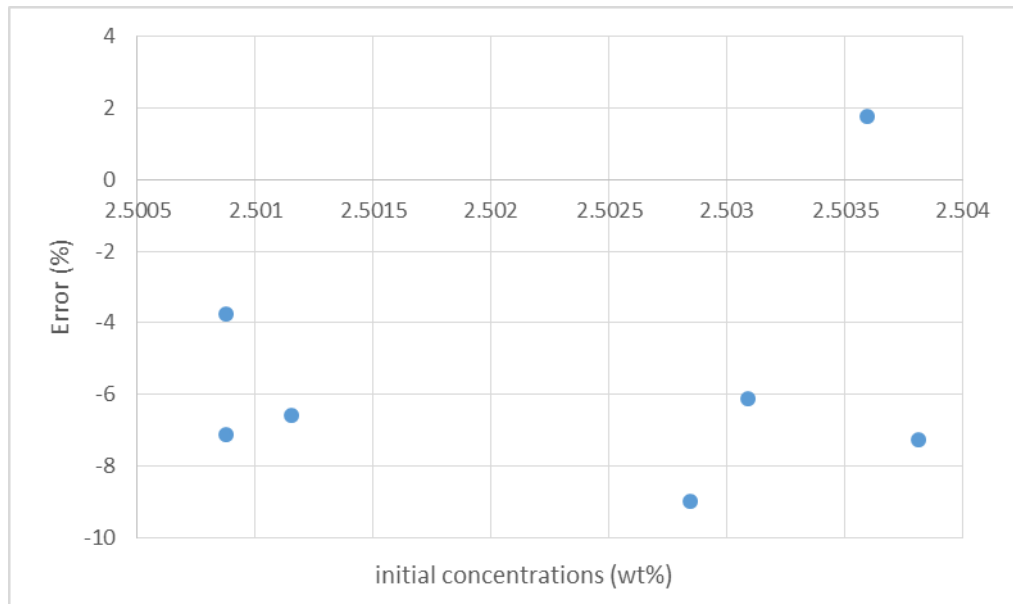


Figure A.1 : Differences between initial concentrations and titration measurements.

Appendix B : Details of a Mass and Component Balance of Filtration for H_3BO_3

In Step-I, 2.49 wt% boric acid solution was prepared and 65.61 gram of sample was collected by syringe for concentration determination of the initial solution.

From Step-I to Step-II, cooling was applied to extract energy from to system to initiate nucleation and crystallization. When crystallization of both ice and salt occurred in Step-II, 63.01 gram of solution sample was collected for determining the eutectic concentration.

During Step-III, the system was operated in the crystallizer under eutectic conditions for 20 minutes. Due to inefficient mixing, some ice and salt crystals grew on the beaker surface as a scaling layer. At the end of Step III, samples from bulk ice, solution and scaling layer were collected for further analysis.

Density of boric acid-water system;

$$d_{\text{water}}=0.997 \text{ g/cm}^3,$$

$$d_{\text{boric acid}}= 1.435 \text{ g/cm}^3 ;$$

$$d_{\text{mixture}}= (0.997 \times 0.975) + (1.435 \times 0.025) = 1.00795 \text{ g/cm}^3 = 1007.95 \text{ g}$$

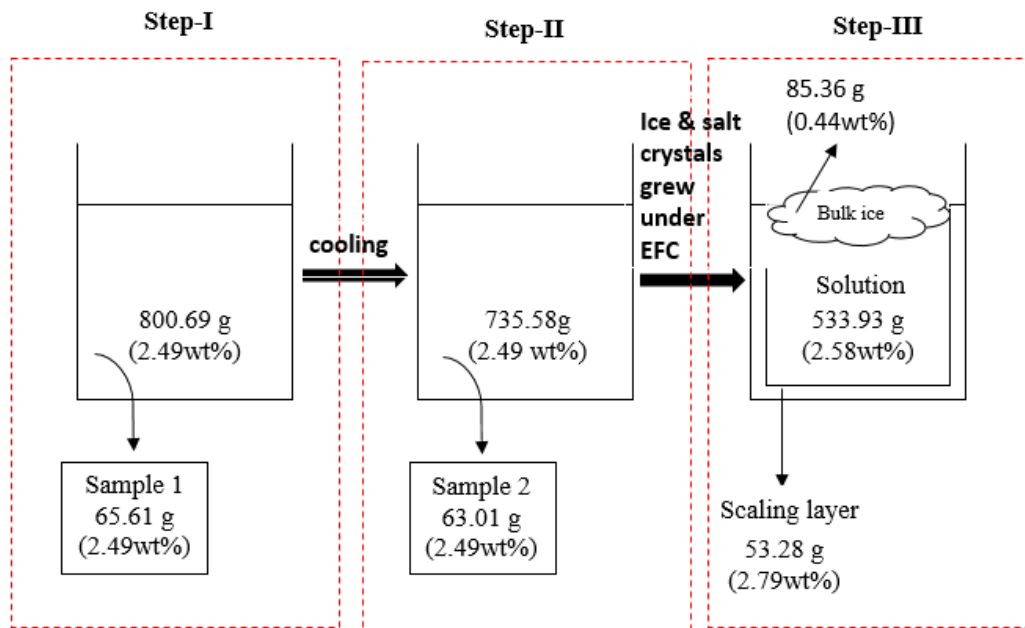


Figure B.1 : Experimental steps before filtration.

Table B.1 : Mass and component balance.

Mass Balance	
Before Filtration	
Input mass (g)	735,58
Sample amount (g)	63,01
Filtrate amount (g)	533,93
Ice amount on the filter (g)	85,36
Ice and salt amounts around the crystallizer (g)	53,28
After 1 st washing	
Filtered ice amount before sampling (g)	85,36
Sample amount (g)	12,3
Washing water amount (g)	50
Filtrate amount (g)	65,65
Amount of ice after washing (g)	57,4
After 2 nd washing	
Filtered ice amount before sampling (g)	57,04
Sample amount (g)	7,83
Washing water amount (g)	50
Filtrate amount (g)	55,04
Amount of ice after washing (g)	44,53

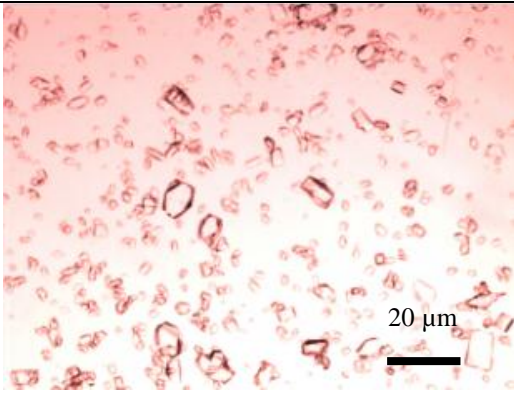
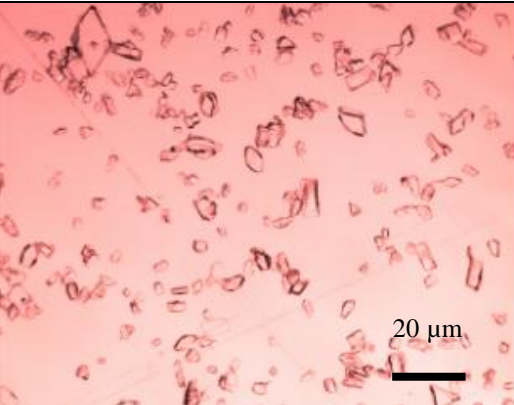
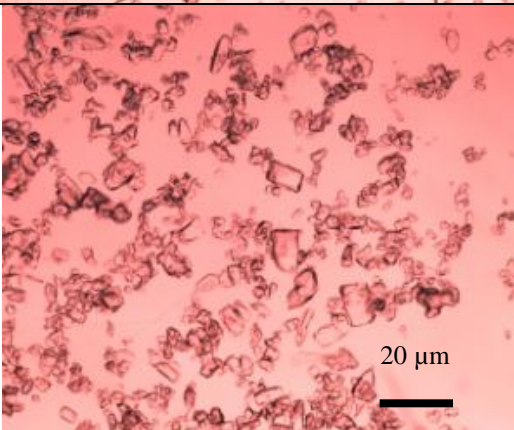
Before Filtration- Total Mass Balance
Input mass = Sample amount+Filtrate+Ice amount on the filter+Ice and salt amounts around the crystallizer
$735,58 = 63,01+533,93+85,36+53,28$
Mass balance is correct.
After 1st washing- Total Mass Balance
Filtered ice amount before sampling = Sample amount+Washing water amount+Filtrate amount+Amount of ice after washing
$85,36+50 = 12,3+65,65+57,4$
Mass balance is correct.
After 2nd washing- Total Mass Balance
Filtered ice amount before sampling = Sample amount+Washing water amount+Filtrate amount+Amount of ice after washing
$57,04+50 = 7,83+55,04+44,53$
Mass balance is correct.

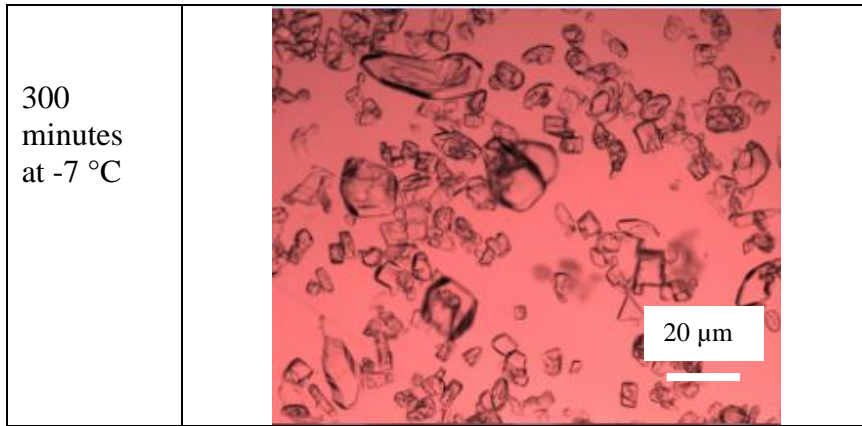
Component Balance –for H₃BO₃	
Before Filtration	
Input concentration (wt%)	2,54
Filtrate concentration (wt%)	2,58
Ice composition on the filter (wt%)	2,22
Ice and salt concentration around the crystallizer (g/l)	27,96
After 1 st washing	
Filtered ice concentration (wt%)	2,2
Washing water concentration (wt%)	0
Filtrate concentration (wt%)	0,98
Concentration of ice after washing (wt%)	1,18
After 2 nd washing	
Filtered ice concentration (wt%)	1,18
Washing water concentration (wt%)	0
Filtrate concentration (wt%)	0,37
Concentration of ice after washing (wt%)	0,83

Before Filtration
Input mass x concentration = (Sample amount x concentration)+(Filtrate x concentration)+(Ice amount on the filter x concentration) +(Ice and salt amounts around the crystallizer x concentration) $735,58 \times (C_1) = (63,01 \times C_1) + (533,93 \times 25.89 \times 100/1007,95) + (85,36 \times 2,22) + (53,28 \times 27,96 \times 100/1007,95); C_1 = 2,54$
No H ₃ BO ₃ loss
After 1st washing
(Filtered ice amount before sampling x concentration)-(Sample amount x concentration) +(Washing water amount x concentration) = (Filtrate amount x concentration)+(Amount of ice after washing x concentration) $(85,36 \times 0,022) - (12,3 \times 0,022) + (50 \times 0) \neq (65,65 \times 0,0098) + (57,4 \times 0,0118)$ $1,62 \neq 1,32$
Amount of H ₃ BO ₃ Loss : $1,62 - 1,32 = 0,3 \text{ g H}_3\text{BO}_3$
After 2nd washing
(Filtered ice amount before sampling x concentration)-(Sample amount x concentration)+(Washing water amount x concentration) = (Filtrate amount x concentration)+(Amount of ice after washing x concentration) $(57,04 \times 0,018) - (7,83 \times 0,018) + (50 \times 0) \neq (55,04 \times 0,0037) + (44,53 \times 0,0083)$ $0,588 \neq 0,244$
Amount of H ₃ BO ₃ Loss : $0,588 - 0,244 = 0,344 \text{ g H}_3\text{BO}_3$

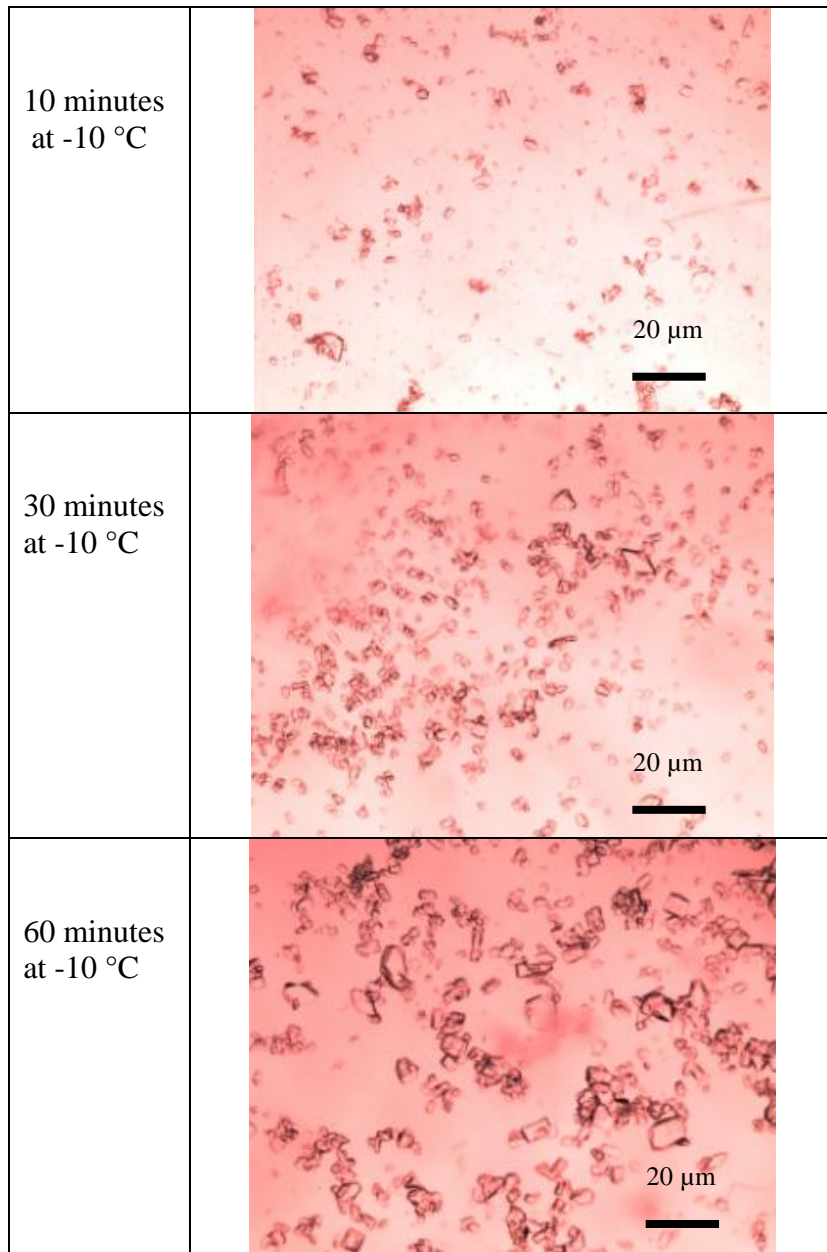
APPENDIX C: Crystal Size Determination experiments' microscopic images for borax decahydrate

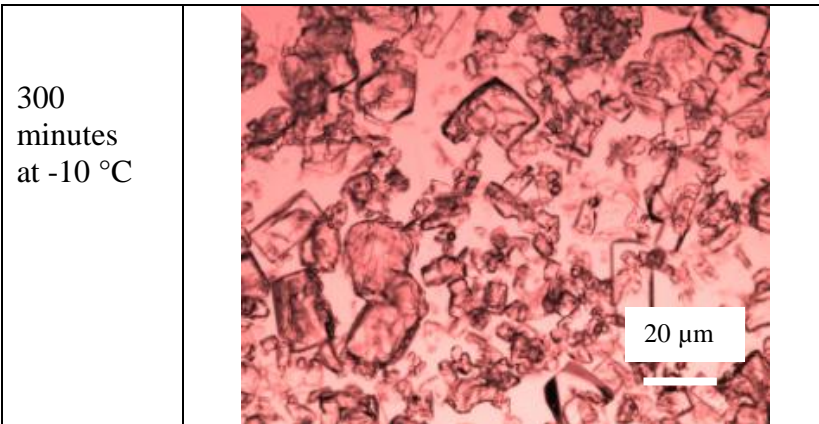
Appendix C.1 : Typical crystal microscopic images visualized using Image Pro Plus software at -7 °C temperature and at different set temperatures.

10 minutes at -7 °C	
30 minutes at -7 °C	
60 minutes at -7 °C	

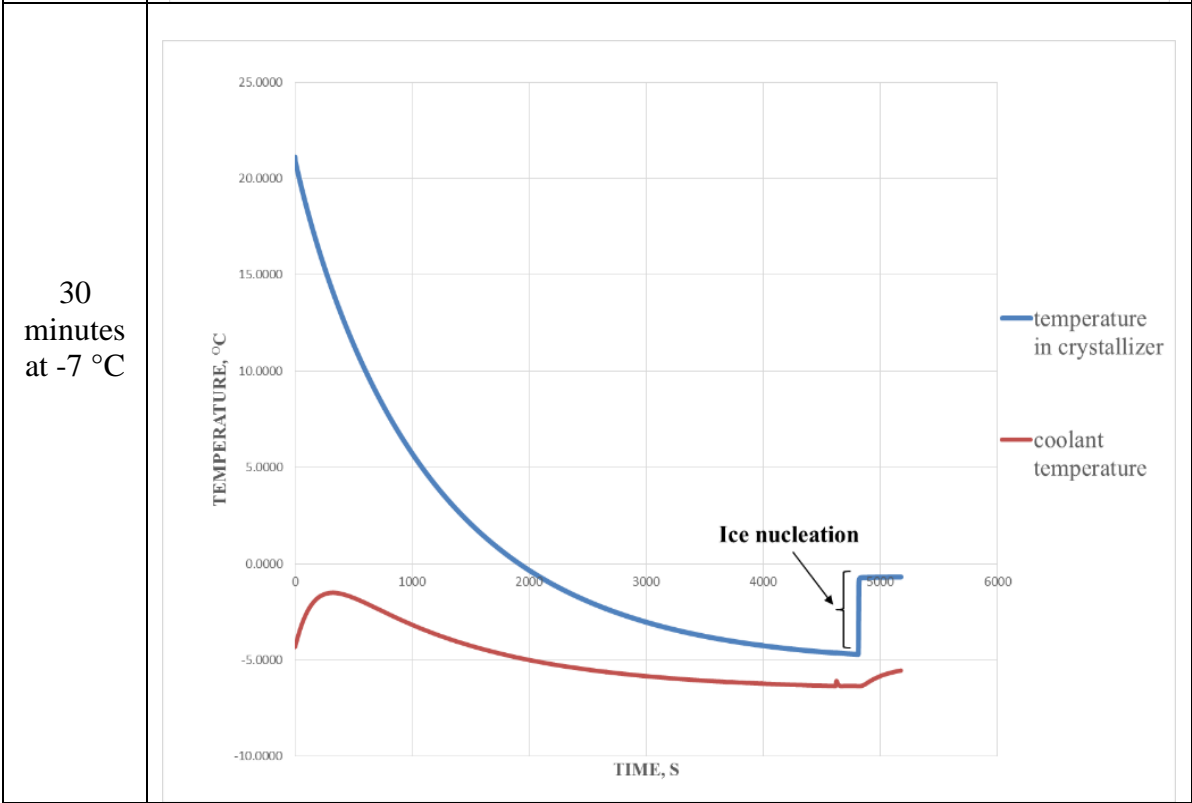
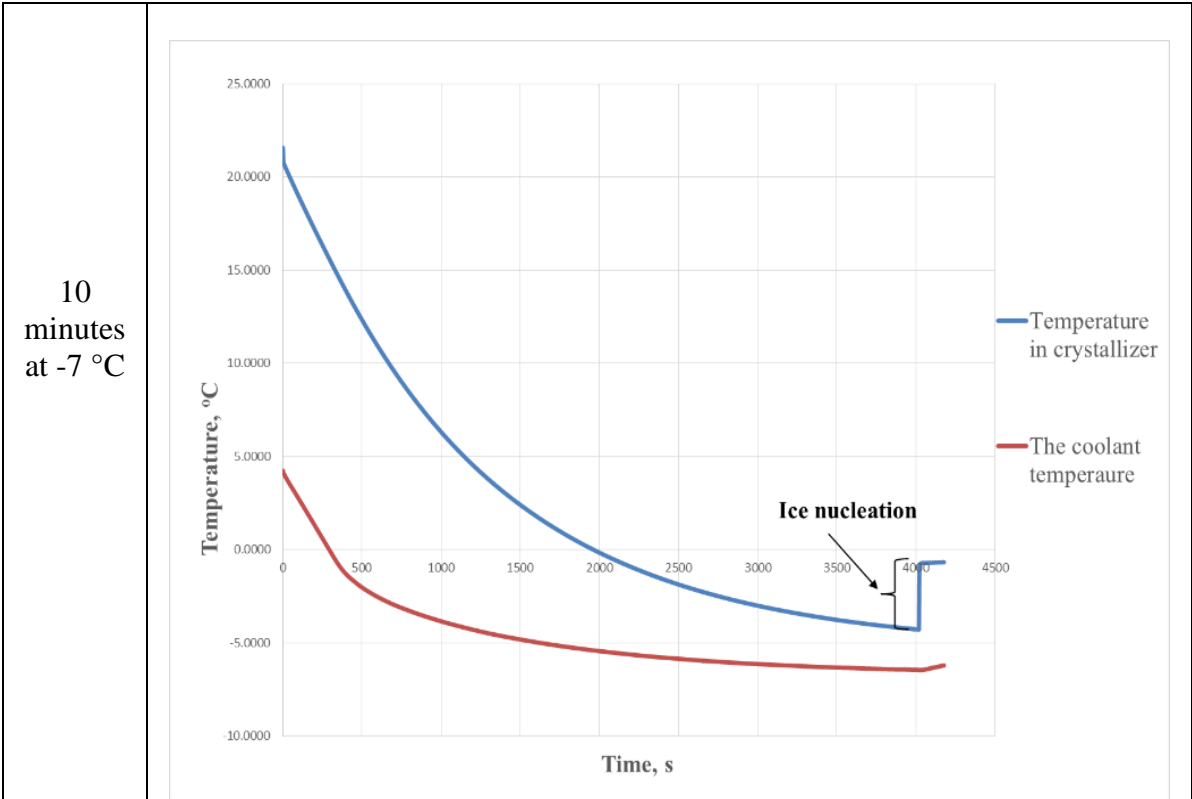


Appendix C.2 : Crystal microscopic images visualized using Image Pro software at -10 °C temperature and at different set temperatures.

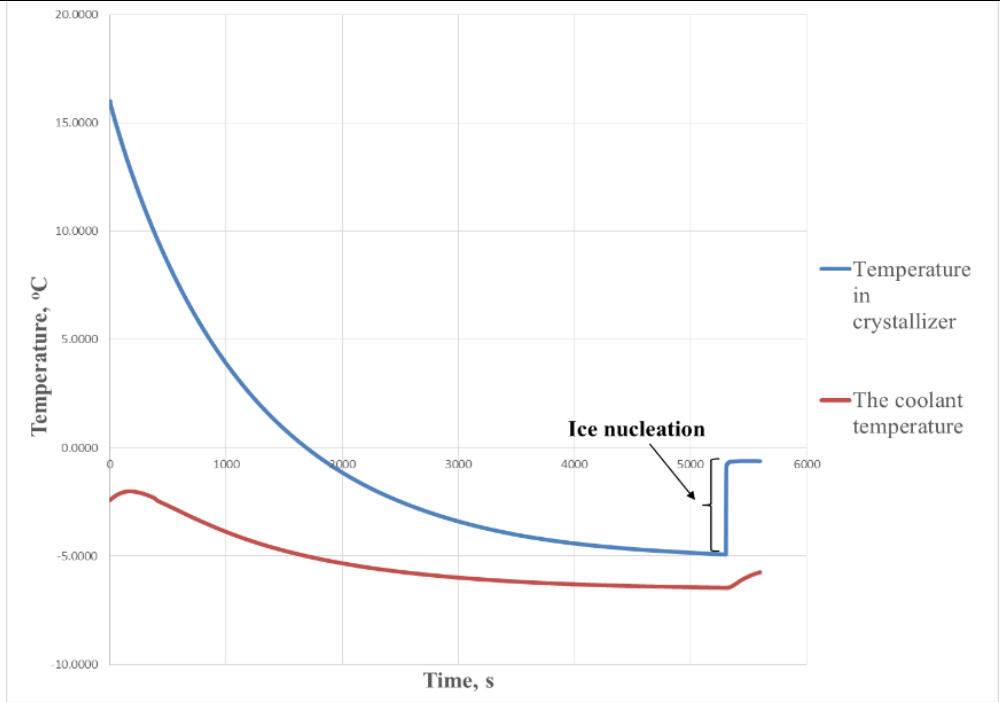




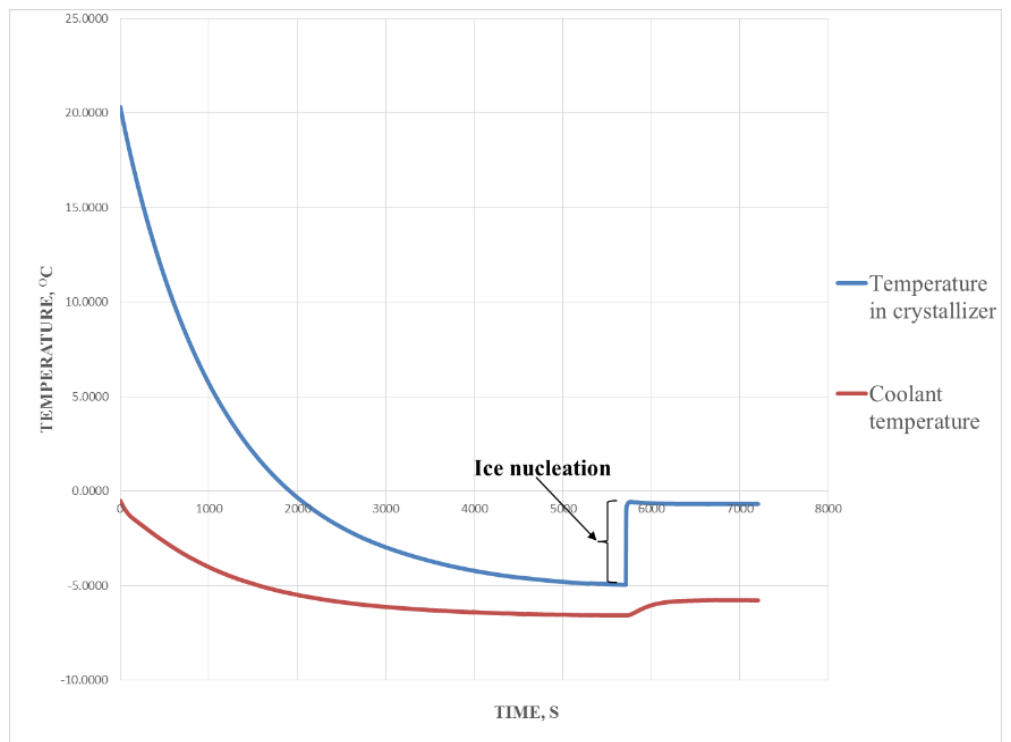
APPENDIX D: Crystal Size Determination experiments' temperature profiles for borax decahydrate



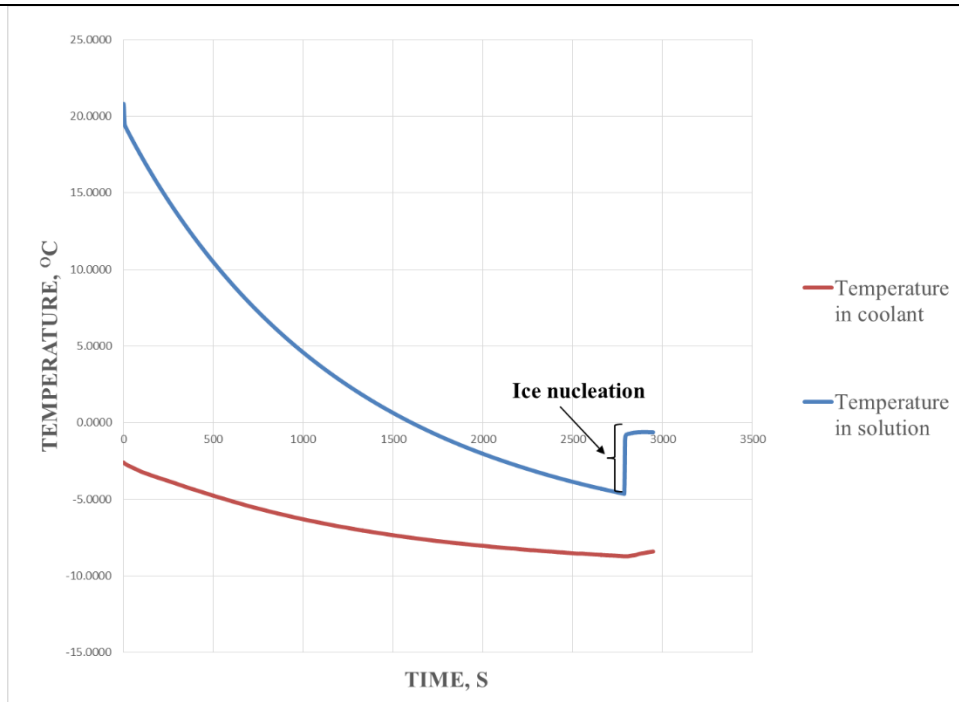
60
minutes
at -7 °C



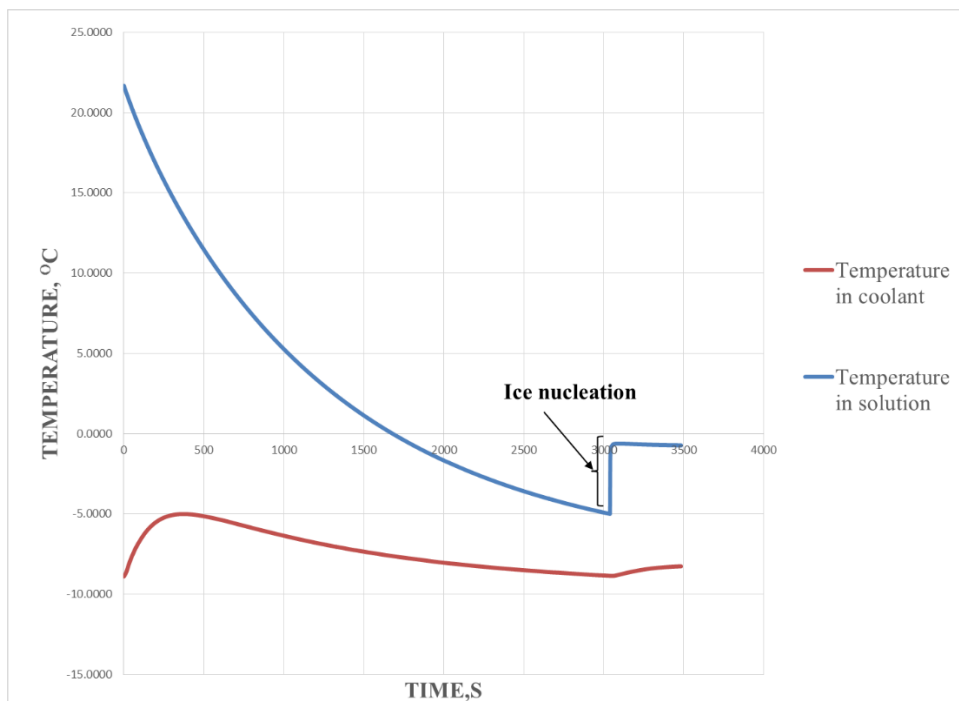
300
minutes
at -7 °C

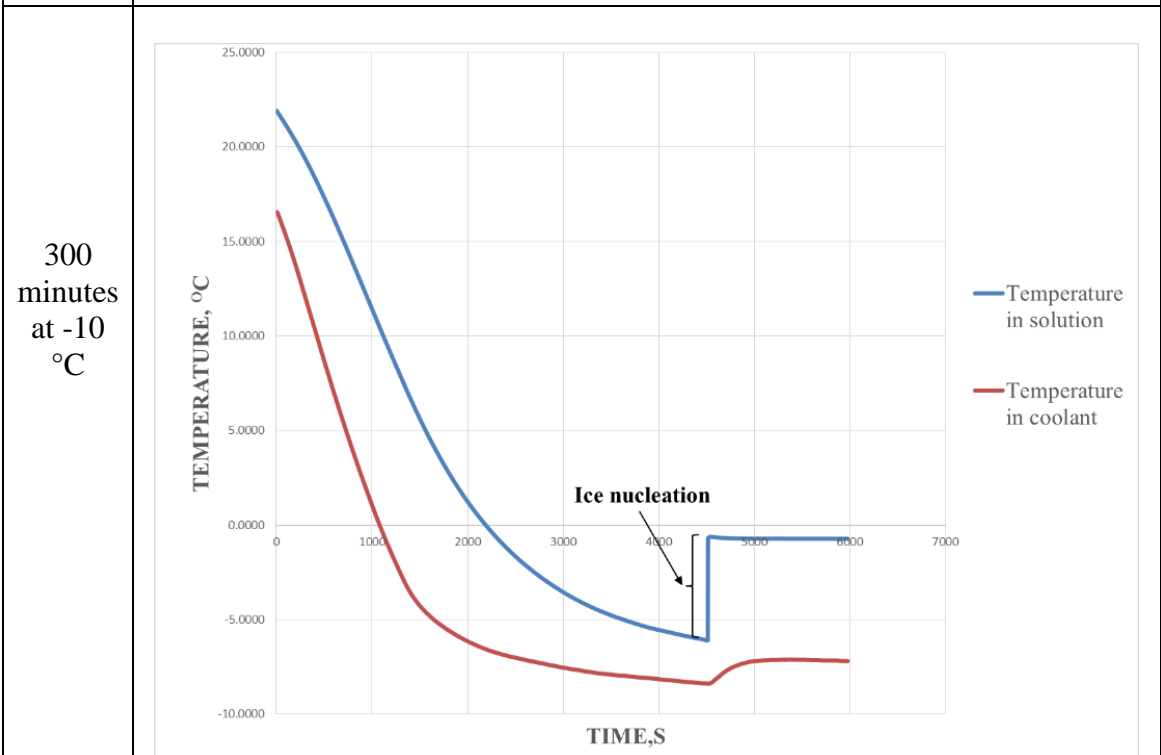
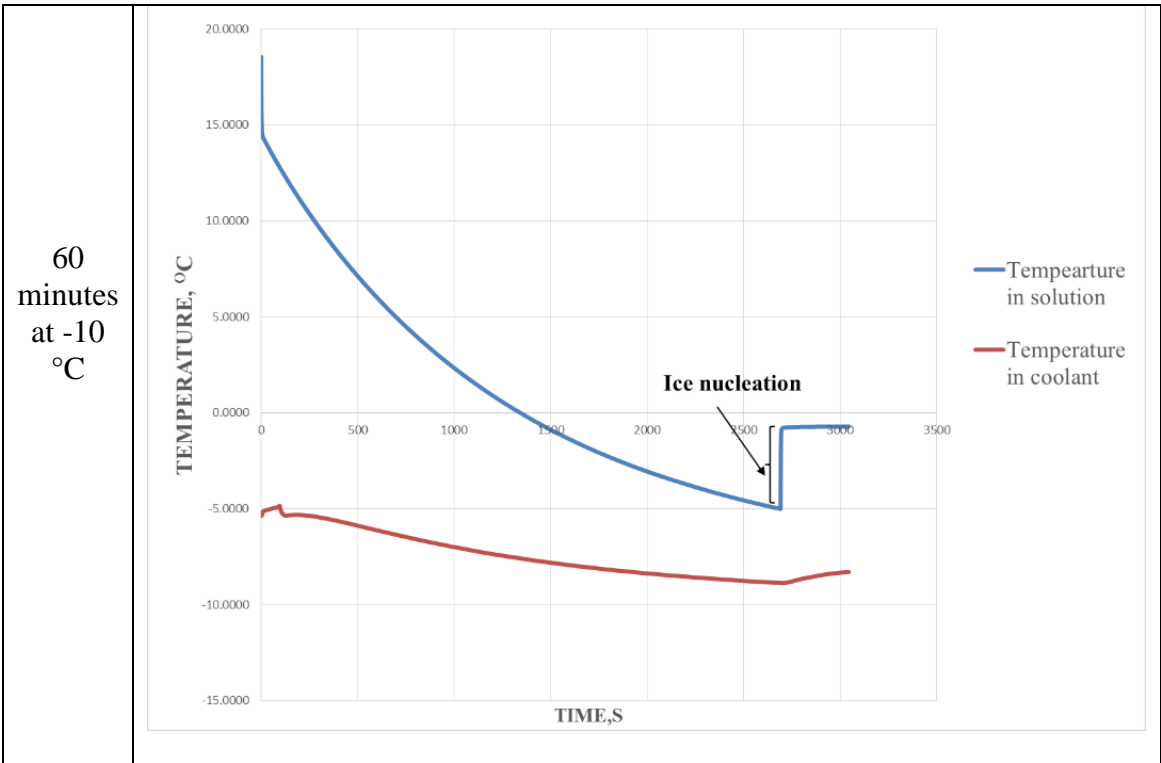


10
minutes
at -10
°C



30
minutes
at -10
°C





CURRICULUM VITAE



Name Surname : Bolormaa BAYARKHUU

Place and year of birth : Ulanbator, 1988

Adress : Çemberlitaş Yurdu, Bindirdirek, 34122 Fatih/İST.

E-mail : bolor2744@yahoo.com

Bachelor Degree : Mongolian University of Science and Technology,
School of Material Science, Organic chemistry.